===== **REVIEW ARTICLE** =====

Mannose Receptors of Alveolar Macrophages as a Target for the Addressed Delivery of Medicines to the Lungs

I. D. Zlotnikov[a] and E. V. Kudryashova[a, 1]

[a] *Department of Chemistry, Moscow State University, Moscow, 119991 Russia*

Abstract—This review was devoted to an investigation of the structure, properties, and functions of the mannose receptors of the alveolar macrophages which were promising targets for the creation of systems of the addressed delivery of medicines for treatment of diseases of the upper airways. In the first section, we discussed a search for an optimal strategy of studies of the ligand-receptor interactions and determination of the ligand specificity to the macrophage mannose receptors with the aim of improving the efficiency and organ bioavailability of drugs. The model proteins for a simulation of the ligand–protein interactions in the in vitro systems were reviewed. The use of concanavalin A as a model mannose-specific lectin allowed a determination of the binding parameters for ligands of different structure, a wide screening of the ligand array, and studies of the contribution of steric factors during the ligand binding. The latter was difficult in the case of such a complex target as the mannose receptor of the alveolar macrophages (CD206). This receptor is inaccessible, and adequate screening in vitro was technically difficult for them. In the second section, we described methods for determining the binding parameters of the carbohydrate-containing ligands to receptors and model lectins: IR spectroscopy, fluorescent methods, affinity chromatography, confocal microscopy, flow cytometry, X-ray analysis, and calorimetry. A large array of quantitative parameters of the complex formation of the oligosaccharide ligands with concanavalin A was analyzed. Selection of the optimal structure of the ligand by varying the density and the number of the mannose-containing ligands, and the spacer length, is considered as a basis for creation of the addressed delivery systems. The practical application of the described approaches to the creation and trials of the addressed delivery of the bioactive substances in the in vivo systems is discussed in the third section of this review.

INTRODUCTION

The increase in the number of the infections which are caused by pathogenic bacteria presents a considerable threat to society and is the main reason for mortality in developing countries and a serious problem for advanced countries. Various highly effective antibacterial medicines are often characterized by a low penetrability through cellular membranes, and their concentration inside a cell does not achieve their level in blood. Therefore, intracellular infections have long been treated with high doses of therapeutic agents. Such treatment results in undesired side reactions and low therapeutic compliance by patients and, thus, increases the risk of developing antibiotic resistance in microorganisms. The formation and development of resistant and multiresistant strains of infectious agents which are simultaneously resistant to several types of antibiotics result in diseases which are poorly treatable with the known medicines. This problem is the most acute in the case of persistent infections or such severe diseases as tuberculosis, pneumonia, and listeriosis, which can give rise to such complications as meningitis, pneumonia, and sepsis. The standard course of tuberculosis treatment involves 4—5 medicines and lasted for 6—12 months. The antituberculous therapy has serious limitations due to an intake of many drugs and the toxic effects that are associated with them. Many of the presently used antibacterial medicines have the stability and bioavailability restrictions, pronounced side effects, and nonoptimal pharmacological properties and can cause damage to the liver and other organs. These problems can be solved by the cre-

---

Abbreviations: AM, alveolar macrophage; DC, dendritic cell; ITC, isothermal titration calorimetry; MR, mannose receptor; MPh, macrophage; FC, Flow cytometry; PEI, polyethylenimine; ATD, antituberculous drug; CD, cyclodextrin; CLSM, confocal laser scanning microscopy; ChitMan, mannose-modified chitosan; ConA, concanavalin A; CRD, Carbohydrate-recognizing site; CTLD, C-type lectin-like region; CysRD, cystein-rich region of MR; diMan, 3-O-(α-D-mannopyranosyl)-D-mannose; FITC, fluorescein isothiocyanate; MBL-A, mannan-binding lectin A; MeMan, methy-α-D-mannopyranoside; MeUmb, methylumbellilferyl; NCs, nanocarriers; ODN, oligodeoxyribonucleotide; PRR, pattern recognition receptor; TLR, Toll-like receptor; triMan, trimannoside.

[1] Corresponding author: phone: +7(915)087-32-67; e-mail: helena_koudriachova@hotmail.com.

ation of novel effective antibacterial medicines and carriers for them with the function of addressed delivery. The mannose macrophage receptors can be a promising target. Macrophages play a key role in the immune response to a number of diseases, including oncological, autoimmune, infectious, fibrotic, and other pathologies. The large number of the mannose receptors (CD206) that mediate endocytosis through the clathrin-dependent mechanism is expressed on a surface of activated macrophages. One of the main functions of the mannose receptors is recognition of patterns of the terminal mannose residues: *N*-acetyl-glycosamine and fucose. They are present on the glycan chains of the surface proteins of several pathogenic microorganisms, including *C. albicans*, *Mycobacterium tuberculosis*, *Pneumocystis carinii*, *Listeria monocytogenes*, *Leishmania donovani*, and others. In addition, the mannose receptors participate in a process of the antigen presentation, resolving of an inflammation, and clearance of several hormones. Therefore, the target action on macrophages could be open new opportunities for an influence on biochemical processes in which these cells are involved. Thus, potential areas of an application of the systems of the target aiming to the macrophages can involve a delivery of antivirus and antibacterial medicines in a nidus of a latent infection for the more effective therapy of such infections as, for example, tuberculosis, HIV, Ebola virus disease, etc.

ALVEOLAR MACROPHAGES AND THEIR RECEPTORS

Alveolar Macrophages

The alveolar macrophages (AMs) are the first "guards" of the respiratory tree. They play a key role in the fight against lung diseases and protect the lung tissue from damages by the recognition and killing of pathogens. AMs release various secretory products which, in their turn, cause phagocytosis and/or the phagolysosome-directed pinocytosis in response to the microorganism invasion [1]. The phagocytosis is blocked during an infection by the tuberculosis mycobacterium, and the cells begin to serve as a refuge for the location and growth of the bacteria. Therefore, the efficacy of antibiotic therapy is strongly limited. The most part of the known antituberculous drugs are weakly effective against the dormant infection (tuberculosis). Thus, the addressed delivery to AMs is of considerable interest for an increase in the efficacy of a medicinal therapy of the respiratory diseases [2].

The Toll-like receptors (TLRs), which are transmembrane glycoproteins [3], play a key role in the macrophage interaction with bacteria. MPhs recognize bacteria, in particular through binding to TLR2 (CD282) and TLR4 (CD284). Arabinomannan, galactomannan, and such components of the bacterial cellular wall as lipoteichoic acids are ligands of these

two receptors on a surface of *Mycobacterium tuberculosis*. Complexes of fragments of TLR2 and TLR4 with the lipoteichoic acid from *Streptococcus pneumoniae* and the lipopolysaccharide from *E. coli*, respectively, are presented in Fig. 1. In the first case, hydrophobic interactions of the fatty acid residues with the Val, Leu, Pro, Phe, and Tyr residues take place. The binding of a carbohydrate to TLR4 occurs mainly through basic and aromatic residues. The receptors activate the MPh signal pathways and induce a secretion of anti-inflammatory cytokines, chemokines, and antimicrobial molecules that kill bacteria or cause the granuloma formation [4−6].

The lectin receptors are another important class of receptors that mediate recognition of pathogens by macrophages (MPhs) and dendritic cells (DCs). The activity of these receptors depends on the presence and concentration of Ca^{2+} ions [7, 8]. The receptors are expressed in many vitally important human organs, including the liver, spleen, lungs, bone marrow, the brain, and in the dendritic cells which are present in blood and lymph [9]. The MPh and DC mannose receptors recognize glycoproteins of microorganisms (for example, *Candida albicans*, *Pneumocystis carinii*, and *Leishmania donovani* [9, 10]) and fungi with the terminal mannose residues. On the contrary, the human glycosides on the unreducing termini are protected with sialic acids. Let us discuss the most important C-lectin receptors (Table 1) of myeloid cells and macrophages, including the CD206 mannose receptor that is of special interest for this article [9, 11, 12].

Mannose Receptors

CD206 (Fig. 2a) is a transmembrane protein (175 kDa) that recognizes glycosylated lysosomal enzymes and carbohydrate fragments with the terminal residues of Man, Fuc, and GlcNac [9, 11, 13]. The *N*-terminus of CD206 involves one cysteine-rich region (CysRD), the fibronectin II domain (FNII, Fig. 2b), and eight lectin-like domains of the C-type (CTLDs [14]). The *C*-terminus of MPhs contains a transmembrane domain and a short *C*-terminal cytoplasmic domain (45 amino acid residues) [11].

Fibronectin is a large extracellular matrix glycoprotein that consists of several domains, including two modules of type II (FN-1 and FN-2), which can bind collagen (gelatin). The FNII domains (Fig. 2b) are found in various proteins, including matrix metalloproteinases 2 and all the members of the mannose receptors (including CD206) [11]. This domain of the mannose receptor provides a binding to cellular surfaces and various compounds, in particular collagen [15], fibrin, heparin, DNA, and most anionic ligands due to the positive charge. Amino acid residues, which play an important role in the receptor-collagen binding (gelatin models the collagen properties in this case), are shown in Fig 2b. By means of a molecular interaction of the collagen binding to this domain, the
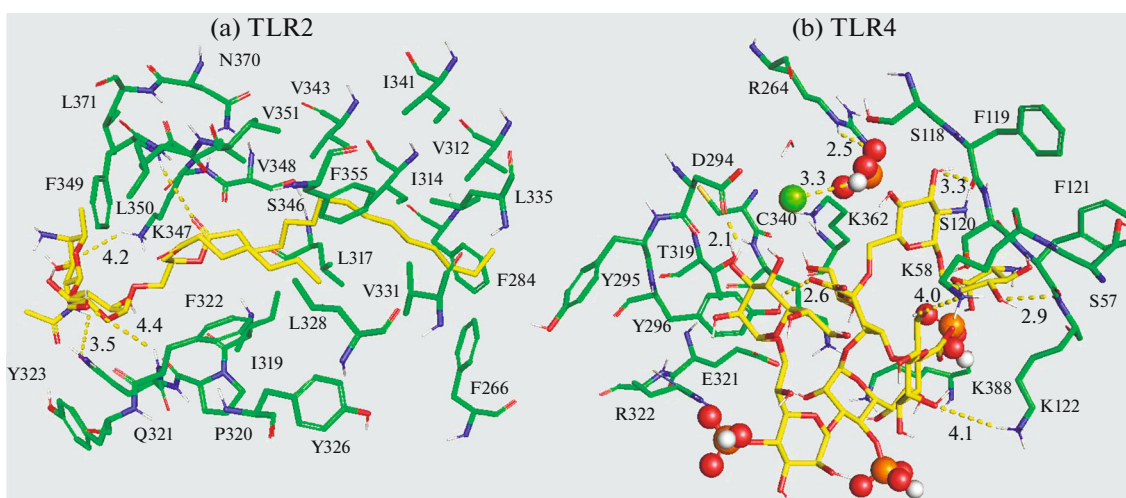
Fig. 1. The Toll-like receptors: (a) TLR2 in a complex with the lipoteichoic acid; (b) TLR4 in a complex with oligosaccharide (PDB: 3a7b, 3fxi). The receptor and the ligand are indicated by green and yellow colors, respectively. The phosphate group are one orange and three red spheres.

aromatic amino acid residues of the domain interact with the collagen amino acid residues in a hydrophobic pocket and disturb the collagen triple helix, whereas the Arg34 and Asp36 residues stabilize this interaction. In addition, the close proximity of the *N*- and *C*-termini allows the formation of a more compact globular structure between the neighboring domains, facilitating the ligand binding. The Phe19, Trp40, Leu17, Tyr21, Phe26, Tyr47, and Tyr53 residues form the hydrophobic pocket [11, 15]. Thus, an energy and specificity of the binding are shown to be increased owing to an aggregation of several receptor domains.

The CysRD domain (Fig. 2a) consists of 147 amino acid residues, contains six cysteine residues, and binds glycoproteins with the terminal 4-sulfo-*N*-acetylglu-cosamine, for example lutropin and thyrotropin.

4-Sulfo-*N*-acetylglucosamine of CysRD has been also shown to form stable hydrogen bonds with the cysteine groups of the mannose receptors [11, 16, 17].

The C-lectin-like region in CD206 involves eight domains of the carbohydrate recognition (CTLDs) (Fig. 2a) [11, 13, 18]. These domains have only 30% homology in the extracellular area of the mannose receptor. The CTLD structures contain two α-helixes and two antiparallel β-sheets. Every of the domains involve amino acid residues that are necessary for binding to Ca^{2+} and ligands. Only regions from the fourth to the eighth (among the all eight regions) are crucially necessary for the binding and endocytosis of the ligands with the terminal Man, GlcNAc, and Fuc. Note that only CTLD4 (its crystalline structure was described by Feinberg et al. [13, 18]) exhibits the

Table 1. Characteristics of the lectin receptors of the myeloid cells and macrophages

Receptor	Structural peculiarities	Specificity to ligands	Cellular location
The mannose receptor (CD206)	Type I, 8 CTLD	Mannose, glucose, *N*-Ac-glucosamine	Immature myeloid dendritic cells, monocytes, macrophages
CD205	Type I, 10 CTLD	Not determined	Immature myeloid dendritic cells, Plasmacytoid dendritic cells, Langerhans cells
CD209	Type II, 1 CTLD	Mannose, fucose	Immature myeloid dendritic cells, mature myeloid dendritic cells, monocytes, macrophages, T-cells
Langerhin (CD207)	Type II, CTLD	Mannose	Langerhans cells
Dectin-1	Type II, 1 CTLD, ITAM	P-Glycan	Immature myeloid dendritic cells, Plasmacytoid dendritic cells, monocytes, macrophages, neutrophils, T-cells
Dectin-2	Type II, 1 CTLD	Mannose	Dendritic cells, Langerhans cells

CTLD, C-lectin-like domain; ITAM, the sequence that is responsible for the cell activation.
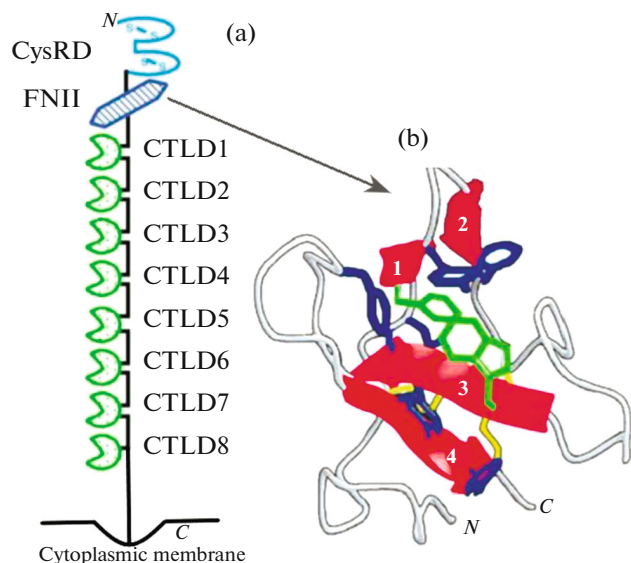
Fig. 2. (a) The structure of the extracellular part of the CD206 mannose receptor. The CTLD4−8 domains are responsible for the binding to the Man residues; (b) the F2 (FN-1F2) domain of the fibronectin−gelatin binding. The 1−4 β-sheets and the disulfide bonds are indicated with the red and yellow colors, respectively. The side radicals of Phe19 and Trp40 are colored in green. The side radicals of Leu17, Tyr21, Phe26, Tyr47, Tyr53, and Phe55 are blue [11].
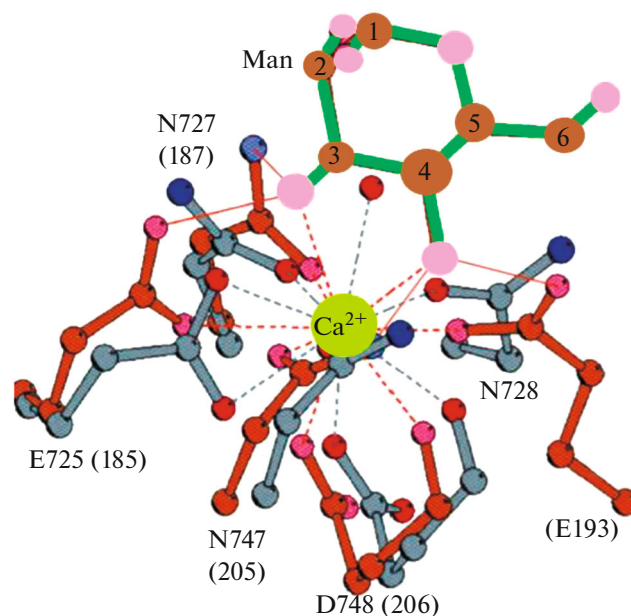

Fig. 3. A comparison of the mannose binding in the presence of the Ca^{2+} ions to the CTLD4 main site of the CD206 mannose receptor (the gray bonds) and the MBL-A receptor (brown bonds). The numbers of the residues are indicated for MR, and the MBL-A equivalents are given in the parentheses [18].

proved carbohydrate-binding activity apart from other domains (i.e., this region itself can recognize the carbohydrate residues, although with insufficient efficiency). The rest of CTLDs are almost devoid of such activity according to the literature data [19, 20]. One should take into account in the course of studies of the ligand-receptor interactions that all the eight domains are necessary for the combined ligand binding with a high affinity and for endocytosis, because the effect of multivalent binding is achieved (the corporative action).

Although all the eight regions play an important role, the fourth region is studied in more detail. The main interaction of CTLD4 with a carbohydrate ligand occurs via a direct binding of Ca^{2+} to the carbohydrate-Ca^{2+}-binding site similarly to the mannan-binding lectin A (MBL-A, PDB: 1MSB) [20, 21]. The mouse MBL-A has an oligomeric structure which consists of two subunits (each subunit of 13 kDa) [22]. The human MBL is a hexamer of trimmers (400−700 kDa) and contains CysRD similarly to CD206 (CTLDs) [23]. This lectin, similarly to MPhs, plays an important role in the inborn immunity and demonstrates the MPh-like mechanisms of the ligand recognition. A comparison of the carbohydrate-binding domains of CTLD4 and MBL is given in Fig. 3 [18].

Since the human MBL is closely examined [23], in particular pathways of its activation and its role in the immune system are studied; this information should be compared with that for the mannose receptor (CD206). Carbohydrate recognition occurs through the cooperation of several CTLDs characteristic of both receptors. They are lectin receptors and have the similar structural motifs. Let us compare functions of these receptors. MBL participates in recognition and binding of carbohydrates on a surface of a cellular wall of microorganisms, resulting in an activation of the lectin pathway of the complement system. In addition, MBL binds apoptotic bodies and increases their phagocytosis. MR recognizes, absorbs, and neutralizes pathogen microorganisms. In addition, MR participates in a production of the anti-inflammatory cytokines that is a basis of the inborn and adaptive immune system.

The pH-dependent and Ca^{2+}-dependent mechanism of the ligand-receptor interaction is characteristic of MR. The receptor affinity decreases by 45 times with the pH decrease from 7.8 to 4.5. The further decrease results in a complete loss of the affinity. The efficacy of the MR recognition of ligands also depends on Ca^{2+}. The interaction begins at the cation concentration $>10^{-4}$ M (the lectin concentration $\approx 10^{-6}$ M), dramatically increases at the concentration $>10^{-3}$ M (this value corresponds to the physiological concentration of Ca^{2+}-ions), and flattens out with the achievement of the maximum affinity [20].

The MBL interaction with a ligand occurs through the lectin pathway. The type of the cascade reaction in

the complement system takes place. Every subsequent reaction occurs due to a chemical functionality that is formed in the previous step. If several binding sites can be formed, every next binding is more stable than the preceding one (the cooperative effect) [24]. The lectin pathway of the complement activation does not require the antibody participation and is induced by a binding of microbial polysaccharides to lectins which circulate in the blood plasma, such as MBL. Moreover, the Ca^{2+}-dependent and pH-dependent mechanisms of the ligand binding analogous to those for MR are characteristic of MBL.

The fourth domain is unique in comparison with the other mannose-binding CTLDs, because the carbohydrate binding to the Ca^{2+}-binding site is supplemented with the carbohydrate interaction with the aromatic ring of Tyr729. This complex interaction increases the binding strength according to NMR studies [11, 13, 18]. The binding with the high affinity is a result of clustering of several CTLDs (sites 1−8 in Fig. 2a) [19]. Such a clusterization allows a binding of multivalent branched ligands, such as highly mannose *N*-connected oligosaccharides of the general formula $(Man)_{0-14}(GlcNAc)_2$. The Man index most often varies from 3 to 9. The cooperative binding is proposed for CTLDs through conformational changes in the receptor in the course of the carbohydrate binding. This aspect is discussed only on the level of hypotheses and common conclusions, and the nature of the effective binding should be studied further, for example, using computer modeling.

CD206 MR plays an important role in the immune response. We confirm this fact by the studies of Suzuki et al. [25]. The CD206 concentration was measured in the blood sera of the patients suffering from tuberculosis and volunteers with suspicion of tuberculosis and proved to be >2000 ng/mL (in average 3000−5000 ng/mL). This parameter was no higher than 1000 ng/mL for healthy people. Hence, the MPh clusters were found in infected regions. The conclusion was drawn that the CD206 level was increased in the blood serum during tuberculosis and could be a potential biomarker for lung diseases [25].

We conclude this section by a summarizing of the functions of the mannose receptors (MRs). The inborn immune system functions in order to protect the host in the first hours after penetration by an infection. This protection is primarily mediated by an activity of phagocytes, such as macrophages. Phagocytes express MRs on their cellular surface. MRs can recognize a wide spectrum of pathogens, including *Candida albicans*, *Pneumocystis carinii*, *Leishmania donovani*, *Mycobacterium tuberculosis*, and *Klebsiella pneumoniae*. MRs have a high potential for use as a target for an increase in the macrophage activation and the recognition of antigens [9, 26]. The location of these receptors precisely on AMs proposes the possibility of the creation of systems of active targeting for treatment of lung diseases, pneumonia, and tuberculosis.

Model Lectins to Identify the Most Specific Ligands: Concanavalin A

The MR interaction of the alveolar macrophages with glycosylated compounds can be investigated using model lectins, in particular, the extensively studied concanavalin A (ConA) [27−32]. ConA is a plant mitogen. It is widely used in biology and biochemistry for the characterization of glycoproteins and other carbohydrate-containing substances on the surface of various cells. ConA (Fig. 4) is specifically bound to definite structures of various sugars, glycoproteins, and glycolipids essentially with unreducing terminal α-D-mannosyl and α-D-glycosyl groups [27−32]. ConA interacts with various ligands which contain the carbohydrates with a large number of Man residues, markers of blood groups, insulin receptors, immunoglobulins, the carcinoembryonal antigen, and the low-density lipoproteins. ConA is used for a purification of glycosylated macromolecules by lectin affinity chromatography and for investigating immune regulation by different immune cells.

ConA is a homotetramer as the majority of lectins and is strongly glycated. Every subunit (26.5 kDa, 235 amino acid residues) binds metal cations (usually Mn^{2+} and Ca^{2+}) and requires their presence for carbohydrate-binding capability [31, 32]. ConA dissociates with the dimer formation at pH ≤ 5.8, but there is no significant difference in the binding parameters of the dimer and tetramer of ConA, i.e., the binding capacity of this lectin is preserved at a higher acidity and even somewhat increased at an acidification of the medium to pH 5, though a small decrease is characteristic of MBL.

ConA interacts with the Man residues of oligosaccharides similar to surface bacterial carbohydrates. Let us discuss the nature of the ligand binding to ConA. The three following residues are involved in the main interactions via the hydrogen bonds: Asp208 with the preceding *cis*-peptide bond (it provides the optimal configuration of the chains), Asn14 which directly interacts with the calcium ions, and Arg228. The whole structure of ConA in a complex with mannose was determined by X-ray diffraction [33] (Fig. 4a). The binding of ConA is similar to that for MR and MBL (Fig. 3), and this lectin is often used as a model for determining the protein−ligand binding parameters. The Van der Waals interactions between the Tyr12, Phe, Leu, or Cys residues are also important. The following conformational changes are observed at the site of the ConA binding. The first change affects the side chain of Arg228, and the second change is revealed as a small transition (~0.5 Å) of the Thr97−Glu102 region [28]. A configuration of the amino acid residues of ConA that are responsible for the binding is predominantly specific towards the mannose structure. The affinity to other monosaccharide residues is
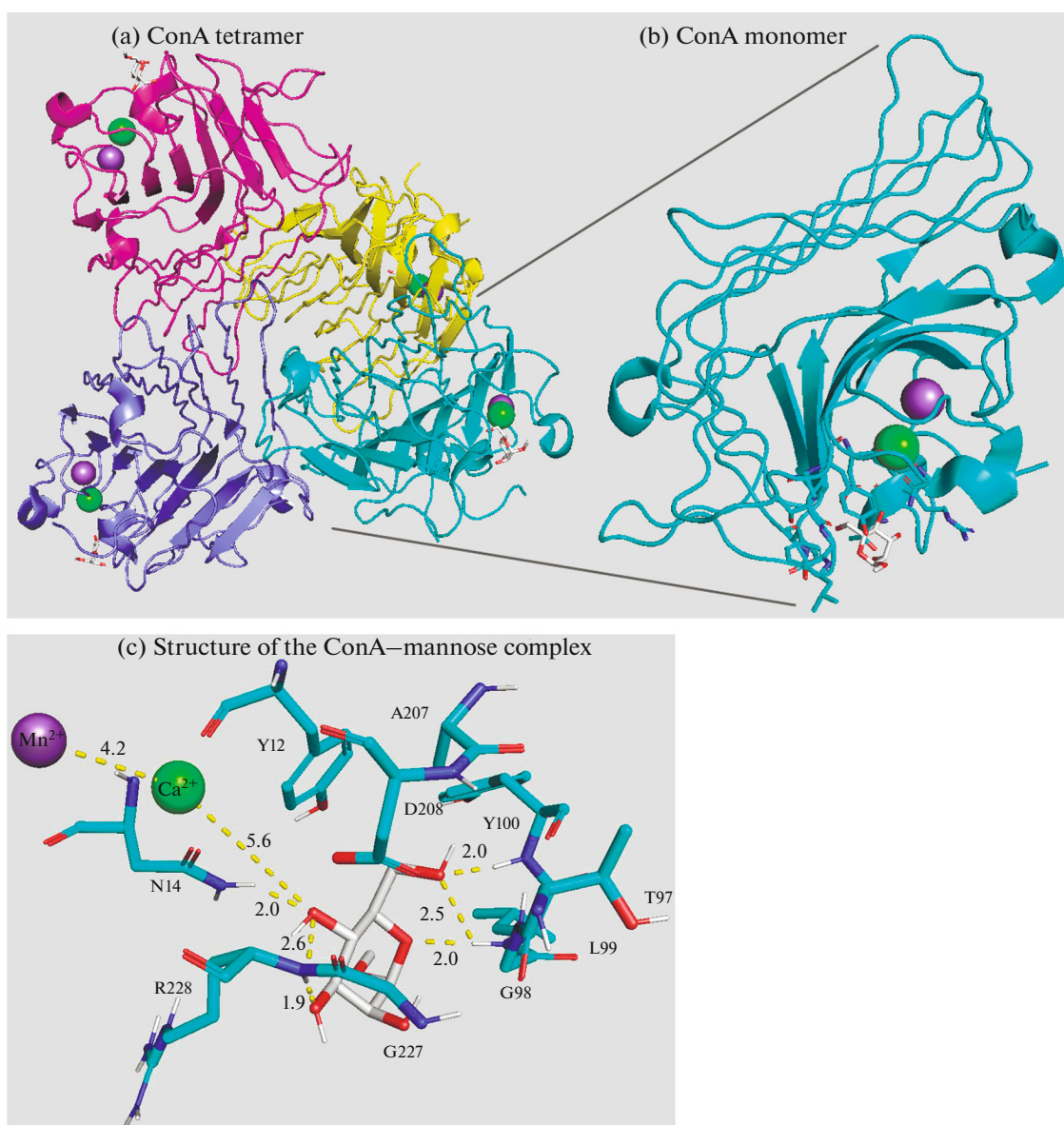
Fig. 4. The structural arrangement of ConA: (a) the tetramer; (b) the enlarged image of one subunit; (c) the ConA complex with mannose. The receptor and mannose are shown by the blue and white colors, respectively. The Ca^{2+} and Mn^{2+} ions look like the green and violet spheres, respectively. The one-letter designations of the residues are given. The distances are expressed in Å.

weaker owing to structural discrepancies between hydroxyl groups of carbohydrates and the binding sites (Table 2).

A scheme of the binding of mannose to ConA is presented in Fig. 4b. It is interesting that ConA does not recognize carbohydrates until the two ion(Ca^{2+}, Mn^{2+})-binding sites are occupied [31, 32]. Ca^{2+} forms coordination bonds with the carbonyl oxygen of the Asn residues, and the side chains are connected with the carbohydrate ligand by the hydrogen bonds. Therefore, the Ca^{2+} "coordination field" fixes the side chains for the optimal interaction with the carbohydrate. The cations also stabilize the lectin sites by a fix-

ation of positions of structural elements of the second shell, i.e., those elements that interact with other protein groups. Mn^{2+} does not coordinate the residues which directly interact with the protein, but fixes the position of Ca^{2+}. The conformational change in the protein which occurs only in the course of its binding to the metal ions is considered to be necessary for the formation of the carbohydrate-binding site [31, 32]. This hypothesis is experimentally confirmed by an analysis of the IR absorption spectra of ConA with different mannose ligands (α-mannose and galactomannan) [34]. ConA specifically binds the residues of α-D-mannosyl and α-D-glucosyl in the terminal position of branched structures of β-glycans, for

Table 2. The values of the dissociation constants (K_d) of the ConA complexes with the carbohydrate ligands, which are calculated at the receptor–ligand ratio of 1 : 1
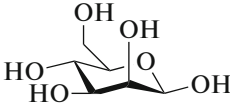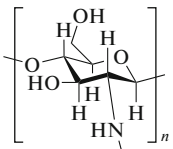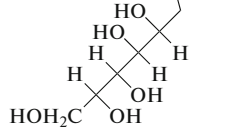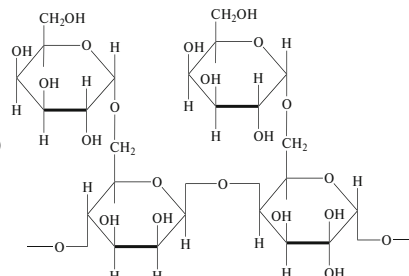
No.	Ligand		K_d of the ConA complex, μM	Conditions, method	Reference
1	Man		350 ± 30	FTIR: changes in IR spectra, pH 7.4, 298 K	[34]
2	ChitMan5		55 ± 3		
3	ChitMan90		16 ± 2		
4	GalMan (200 kDa)		520 ± 40		
5	diMan (dimannoside)		84 ± 8	Opposite titration at pH 5.5, 298.3 K	[45]
6	triMan (trimannoside)		9.1 ± 0.4		
7	MeMan		156 ± 12		
8	MeUmb-Man		23.0 ± 0.3 (29.2 ± 0.4 at pH 5.5)	The fluorescence quenching at pH 7.2, 298.3 K	[44]
9	MeUmb-diMan		7.2 ± 0.3		
10	MeUmb-triMan		12.2 ± 0.4		
11	Me-α-Glc		510	Isothermal titration calorimetry at pH 7.2, 298 K	[47]
12	Me-α-GlcNAc		930		
13	Maltose		760		
14	Maltotriose		750		
15	MeMan		122		
16	Me-α2-D-Glc		365		
17	α(1,2)-Mannobiose	Man $\xrightarrow{\alpha1,2}$ Man —OH	2.4		
18	Me-α(1,2)-Dimannoside	Man $\xrightarrow{\alpha1,2}$ Man $\xrightarrow{\alpha1}$ OMe	7.1		
19	α(1,2)-Trimannose	Man $\xrightarrow{\alpha1,2}$ Man $\xrightarrow{\alpha1,2}$ Man —OH	2.6		
20	α(1,3)-Mannobiose	Man $\xrightarrow{\alpha1,3}$ Man —OH	71		
21	Me-α(1,3)-Dimannoside	Man $\xrightarrow{\alpha1,3}$ Man $\xrightarrow{\alpha1}$ OMe	30		
22	α(1,6)-Mannobiose	Man $\xrightarrow{\alpha1,6}$ Man —OH	75		

Table 2. (Contd.)
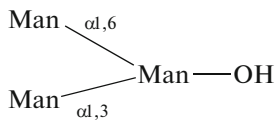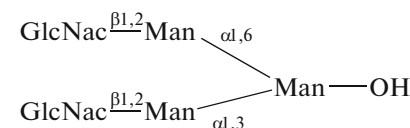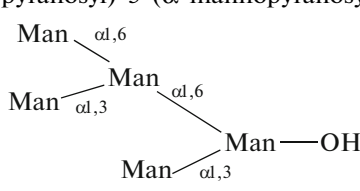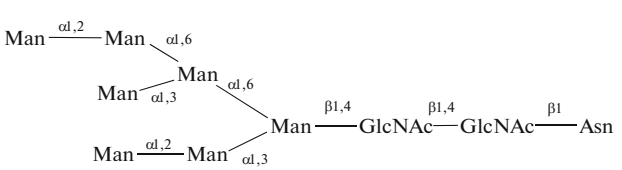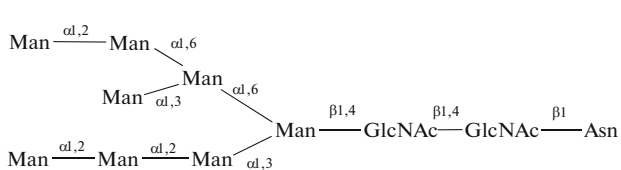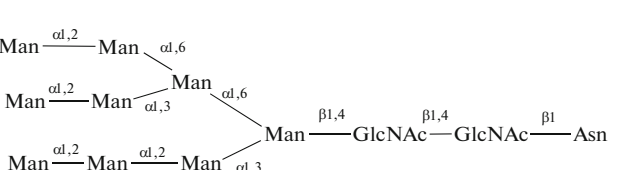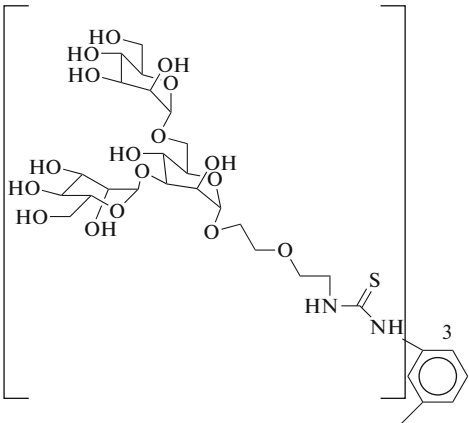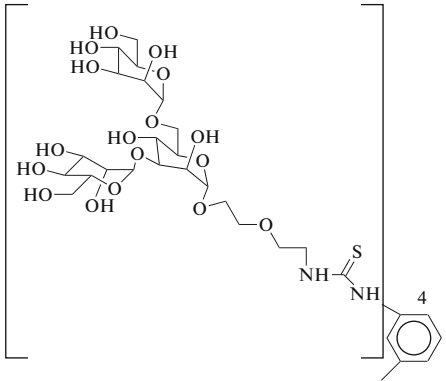
No.	Ligand	K_d of the ConA complex, μM	Conditions, method	Reference
23	Me-α(1,6)-Dimannoside Man —$^{\alpha1,6}$— Man —$^{\alpha1}$— OMe	123	Isothermal titration calorimetry at pH 7.2, 298 K	[47]
24	β(1,2)-GlcNAc-Man GlcNac —$^{\beta1,2}$— Man —OH	150		
25	3,6-di-*O*-(mannopyranosyl)-α-mannopyranose Man $^{\alpha1,6}$ / Man $^{\alpha1,3}$ — Man —OH	3.0		
26	Me-3,6-di-*O*-(Mannopyranosyl)-α-mannopyranoside	2.0		
27	3,6-di-*O*-(β(1,2)-GlcNAc-mannopyranosyl)-α-mannopyranose GlcNac —$^{\beta1,2}$— Man $^{\alpha1,6}$ / GlcNac —$^{\beta1,2}$— Man $^{\alpha1,3}$ — Man —OH	0.71		
28	6-(3,6-Dimannopyranosyl)-3-(α-mannopyranosyl)-α-mannopyranose Man —$^{\alpha1,6}$— Man $^{\alpha1,3}$ / Man $^{\alpha1,6}$ / Man $^{\alpha1,3}$ — Man —OH	1.5		
29	Man7-glycopeptide (model) Man —$^{\alpha1,2}$— Man $^{\alpha1,6}$ / Man $^{\alpha1,3}$ / Man $^{\alpha1,6}$ — Man —$^{\beta1,4}$— GlcNAc —$^{\beta1,4}$— GlcNAc —$^{\beta1}$— Asn Man —$^{\alpha1,2}$— Man $^{\alpha1,3}$	3.3 (K_d was determined for the mixture of Man7 and Man8)		
30	Man8-glycopeptide (model) Man —$^{\alpha1,2}$— Man $^{\alpha1,6}$ / Man $^{\alpha1,3}$ / Man $^{\alpha1,6}$ — Man —$^{\beta1,4}$— GlcNAc —$^{\beta1,4}$— GlcNAc —$^{\beta1}$— Asn Man —$^{\alpha1,2}$— Man —$^{\alpha1,2}$— Man $^{\alpha1,3}$			
31	Man9-glycopeptide (model) Man —$^{\alpha1,2}$— Man $^{\alpha1,6}$ / Man —$^{\alpha1,2}$— Man $^{\alpha1,3}$ / Man $^{\alpha1,6}$ — Man —$^{\beta1,4}$— GlcNAc —$^{\beta1,4}$— GlcNAc —$^{\beta1}$— Asn Man —$^{\alpha1,2}$— Man —$^{\alpha1,2}$— Man $^{\alpha1,3}$	0.91		

Table 2. (Contd.)

No.	Ligand	K_d of the ConA complex, μM	Conditions, method	Reference
32		0.24	Isothermal titration calorimetry at pH 7.2, 298 K	[48]
33		0.074		
34	D-Glucose	4070	The Landsteiner inhibition method [*]	[27]
35	D-Mannose	890		
36	D-Fructose	1790		
37	Galactose	>22 500		
38	Allose	(low affinity)		
39	Methyl-α-D-glucopyranoside	510		
40	Methyl-β-D-glucopyranoside	>12 700		
41	Methyl-α-D-mannopyranoside	122		
42	Methyl-*N*-Ac-α-glucosamine	1015		
43	Methyl-α-D-fructopyranoside	>30 000		
44	Methyl-β-D-fructopyranoside	173		
45	Methyl-α-D-fructopyranoside	3200		
46	Methyl-β-D-fructopyranoside	1160		
47	Methyl-α-L-sorbopyranoside	630		
48	Maltose	880		
49	Isomaltose	450		
50	Cellobiose	>22 500 (low affinity)		
51	Laminaribiose			
52	Genciobiose			
53	Sucrose	4710		
54	Sophorose	1420		
55	2-*O*-β-D-Galactopyranosyl-D-glucose			
56	Methyl-α-sophoroside	245		

* The K_d values of ligands nos. 34–56 were calculated relatively to Me-α-Man (ligand no. 15).

example, mannoglucan or glucomannan. ConA has four binding sites that correspond to four identical subunits.

Liener et al. [27] studied the influence of the structural organization of a ligand on the stability of the complexes and determined the affinity of monosaccharides and oligosaccharides to ConA. The dissociation constants (K_d) of the complexes of carbohydrate ligands nos. 34–56 with ConA are given in Table 2 (the constants were calculated relatively to the MeMan etalon). Disaccharides (for example, maltose and isomaltose) were found to be bound slightly better than mannose. The methyl derivatives of carbohydrates often have a better efficiency. A deterioration or improvement of the binding depend on a spatial orientation of the hydroxyl group (α or β), and the difference can achieve 1–2 orders. ConA is more preferably bound to α-D-mannopyranosides than to the corresponding β-anomers [27]. However, the opposite picture is observed in the case of fructose.

The most specific monosaccharide ligand from the paper of Liener et al. [21] was methyl-α-mannopyranoside which was seven times more effectively bound to ConA than mannose. Titov et al. [35] confirm this fact in the review article [35] that was devoted to the determination of the binding efficiency of ConA to free anomers and their glycocluster conjugates with cyclodextrin. The ELLA method (an analysis of lectin that was based on a competitive binding of ligands to the enzyme-labeled lectin) demonstrated that the conjugates of β-cyclodextrin and the mannose residues without a spacer did not inhibit the lectin binding to mannan (from *Saccharomyces cerevisiae*) and did not compete for the ConA binding sites, because the conjugate affinity was significantly lower than that of mannan. On the other hand, the conjugates with a spacer (2-mercaptoacetamide, thiourea, and ethane-1,2-dithiol), the presence of which is necessary for overcoming the steric hindrance, demonstrated the strong binding to ConA and proved to be 16–17 times effective than methyl-α-D-mannopyranoside. The mannose residue in the conjugate with the spacer was shown to be ~2.4 times more active than the univalent methyl-mannoside. The main role in the increase in the binding strength is played the spatial organization and structure of the mannose ligands. A promising way for improving the binding efficiency was use of the spacer of optimal length, which would provide a balance between the density of the mannose ligands and the absence of steric hindrance.

Thus, ConA is an available and relevant model object for studies of interactions of the mannose receptors of AM with different ligands, because ConA is an available natural compound that allows the determination of the binding parameters without the complex in vitro and ex vivo experiments with MRs themselves.

Modern analytical methods must be used for the ligand–receptor investigations. Such methods are described in the next section. It should be noted that development of modern technologies creates the possibility to obtain reliable data on the intermolecular interactions which directly determine the binding mechanism, on structures of ligands and proteins, and on expression of receptors on the AM surface.

DETERMINATION OF THE BINDING PARAMETERS OF CARBOHYDRATE LIGANDS WITH MANNOSE RECEPTORS AND MODEL LECTINS

Fast and well reproducible methods for the determination of parameters of the receptor–ligand binding are necessary for an analysis of properties of synthesized carriers with the function of the addressed targeting to the mannose receptors of macrophages. In the next section, we discuss the methods for an analysis of these interactions and compare characteristics of the methods.

IR-Fourier-Spectroscopy: Attenuated Total Reflectance (FTIR-ATR)

IR spectroscopy is a promising method for an investigation of the protein–ligand interactions. This method allows a determination of the features of a structure, active sites, and spatial orientation of molecules, evaluation of conformational changes in proteins, and measurements of the K_d values of the ligand complexes [34]. Advantages of the IR-Fourier spectroscopy in the regime of the frustrated total internal reflection (FTIR-ATR) are high sensitivity and an application of small amounts of the analyzed substance. This method does not require optical transparency of the sample, and the protein spectrum can be recorded in a suspension, in an aggregated state, or in composition with membrane fragments.

This method is widely applied in the analysis of the secondary structure of a protein. The Amide I band (a contribution of the valent vibrations of the C=O and C–N bonds are 80% and ~15%, respectively) and the Amide II band (the main contribution of the deformation vibrations of the N–H bonds is ~80% and the minor contribution of the valent vibrations of the C–N bond is ~15%) are of a special importance in the IR spectrum of the protein (Fig. 5), because these bands correspond to the vibration of a peptide bond [31]. The Amide I area of the spectrum (1600–1700 cm^{-1}) is of great interest, since precisely this area is the most sensitive to changes in the protein secondary structure.

Naismith et al. [36] and Gerlits et al. [37] have revealed the changes that occur in the secondary lectin structure during the binding to the mannose ligands (this data is described in the X-ray analysis section in detail) by X-ray analysis and neutron crystallography.

The influence of these conformational changes on the IR spectrum of lectin is illustrated in Fig. 5. The formation of hydrogen bonds during an arrangement of the protein secondary structure results in a change in energy of the vibrations of the peptide bonds. Bands that correspond to the valent vibrations of the N−H and C=O bonds are shifted in the low-frequency area of a spectrum (the area of the lower energies), because the presence of a hydrogen bond facilitates a displacement of the nitrogen atom of the amide group and the oxygen atom of the carbonyl group to the direction of an acceptor or a donor of a proton, respectively, causing changes in the state of α-helixes. The Amide II absorption area is shifted to the high-frequency area, because the hydrogen bond prevents a deformation of the N−H bond. Moreover, a decrease in the intensity of the Amide II band is observed due to the formation of hydrogen bonds and Van der Waals interactions. As a result, a screening of regions of the peptide chains in the binding site occurs, the water-mediated ligand–protein interactions are weakened, and stability of the complex is increased in comparison with the receptor. The absorption intensity in the area neighboring Amide II dramatically increases mainly owing to a cophase combination of a flexure in the plane of the N−H bond and a deformation vibration of the tension of the C−N bond, because these bonds are very sensitive to the secondary structure. These events allow a conclusion about the change in the microenvironment of the peptide chain and β-sheets, and X-ray analysis confirms this conclusion [36, 37].

Sukumaran [38] analyzed the secondary structure of ConA by IR spectroscopy. The characteristic Amide I and Amide II bands of the protein structures were used among the analytically important peaks. The ConA secondary structure was determined on the basis of the spectra. The lectin contained 42% of the β-sheets and 4% of the α-helixes. Differences in the composition of the secondary structure between the X-ray data and FTIR data are small and are explained by physicochemical state of the protein samples (the crystalline state in comparison with the solution, temperature, and pH). Thus, this method is promising for a determination of the structure of biopolymers and lectin–ligand complexes. IR spectroscopy can demonstrate that the Ca^{2+} and Mn^{2+} cations play an important role in the protein–ligand interaction, as mentioned above. Le-Deygen et al. [34] found that the complex formation with the mannose-containing ligands resulted in uniform changes in a spectrum of the examined protein (Fig. 5), in particular, a decrease in the intensity of the Amide II absorption band in the Amide-I-normalized spectra. The authors concluded on the basis of these results that the binding with the mannose-containing ligand would be the most effective at a definite conformation of ConA, which was formed at the specified concentration of Ca^{2+} and Mn^{2+}.
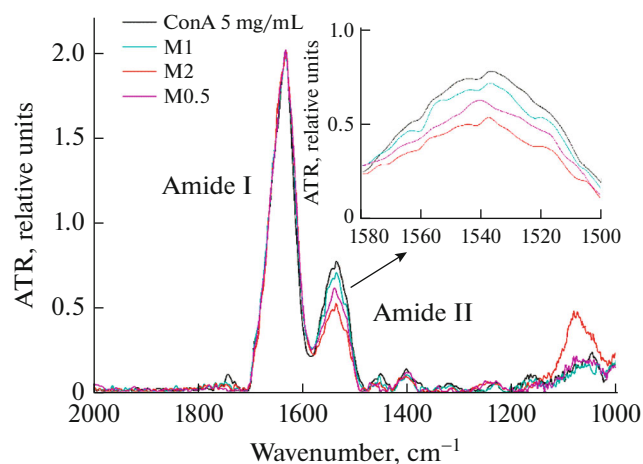

Fig. 5. The IR spectrum of ConA and its changes during the binding of the different ConA/mannose ratios. The number after M indicates the concentration ratio between Man and ConA [34].

In addition to a revelation of the changes in the protein secondary structure, IR spectroscopy can quantitatively determine the affinity of different carbohydrates to lectins. Le-Deygen et al. [34] identified the most specific MR ligands of the alveolar macrophages by this method (the AM binding was modeled using the ConA mannose-specific lectin). For this reason, the ConA conformational changes were analyzed and the binding constants of the mannose-containing medicinal carriers to the lectin were determined on the basis of the IR spectra of ConA and its complexes with the ligands. The following lectin ligands were examined: mannose (Man), ChitMan5 or 90 (chitosan of a molecular weight of 5 or 90 kDa that was modified with the mannose), and galacto-mannan (GalMan) (Table 2; ligands nos. 1−4). A linearization of the isothermal curves of a sorption of the ConA complexes with the mannose-containing ligands allowed a calculation of the K_d values of these complexes.

The branched trimannoside (the mannose three) is a natural ligand for ConA. The K_d value of the complex of this ligand with ConA is 0.26×10^{-5} M. Chitosan (90 kDa) which is modified with mannose by a degree of 20% (ChitMan90) forms the most stable complex with ConA among all the substances that have been analyzed by Le-Deygen et al. [27]. The two-chain chitosan (90 kDa) binds the lectin 3.5 and 22 times more effectively in comparison with ChitMan5 and mannose, respectively, owing to the multipoint interactions with several subunits of the ConA molecule, whereas the short-chain chitosan (5 kDa) does not exhibit such a property, though this molecule also has the multivalent interaction with the receptor. Analysis of the crystal structure (PDB: 5CNA) gives an average distance between the binding sites of carbohydrates to ConA (68 Å). The distance between the terminal resi-

dues of the short-chain chitosan (5 kDa) is no higher than 10−15 Å, whereas it is 170−185 Å for the long-chain polymer. Thus, the long-chain polymers are able to envelop the protein and immediately interact with two of three sites distinct from the short-chain chitosan. Therefore, the efficiency of recognition of the ligand by lectin is dramatically increased.

Galactomannan does not demonstrate a high affinity to ConA and is bound much more weakly than mannose. The mannose residues in galactomannan are generally located in the main chain and their availability is decreased. The content of the terminal Man residues is small. Therefore, the galactomannan binding to ConA is ineffective. The galactose residues are unspecific to the receptor, and the galactose affinity is 25−30 times lower than that of mannose [27]. The mannose residues of ChitMan which is bound to ConA with high efficiency are placed on each side of the main chain and can participate in the interaction with the lectin.

Thus, details of the lectin–ligand interaction are elucidated and the most specific MR ligands are determined on the basis of the results of IR spectroscopic studies.

Fluorescence Spectroscopy

Fluorescence spectroscopy is one of the most common methods for studies of the physicochemical properties of biological systems and, in particular, proteins [39−45]. This method reveals changes in a microenvironment of the protein fluorophores or in an introduced fluorescent label. The tryptophan residues in proteins are mainly responsible for their intrinsic fluorescence. The wavelength range from 295 to 300 nm is used for a selective excitation of the Trp residues. The absorption of Tyr and Phe is minimal at these wavelengths. The Trp fluorescent properties are very sensitive to its microenvironment, especially its polarity. Correspondingly, the complex formation with low-molecular-weight ligands and macromolecules, denaturing, aggregation, and other processes significantly affect the fluorescence spectra of proteins. A shift of the fluorescence maximum and fluorescence quenching can be observed during the protein aggregation or the ligand binding to proteins [39−45].

Let us discuss an application of fluorescence spectroscopy to the determination of the efficiency of the ligand binding to receptors. Landshcoot et al. [44] have studied the relationship between the fluorescence quenching and the ligand binding to ConA. The MeUmb glycosides are prospective ligands for equilibrium and kinetic studies of the carbohydrate−protein interactions. A high absorption coefficient and fluorescence intensity of these glycosides (the maximum emission at 373 nm) provide very sensitive detection. The absorption spectra of these ligands considerably differ in a range from 300 to 350 nm during ligand binding. The fluorescence properties of the ligand are also changed. Pronounced fluorescence quenching is observed in many cases. It is important that the changes are well pronounced and specifically depend on the carbohydrate structure. For example, significant fluorescence quenching of 4-methylumbelliferyl α-D-mannoside (MeUmb-Man) is observed during the binding to ConA. K_d of the complexes, which are determined on the basis of a change in the fluorescence intensity, are given in Table 2 [44]. Trimannoside (triMan) has the maximum binding specificity to ConA among ligands nos. 5−10. However, MeUmb-diMan has the highest affinity among the presented methylated derivatives of umbelliferon. A spatial factor probably plays a role in this case. Three mannose residues are effectively bound, but the additional residue of umbelliferon creates a steric hindrance, and the affinity is decreased.

Later, Landshcoot et al. [45] determined K_d of MeMan, dimannoside (diMan), and trimannoside to ConA in the temperature interval from 285 to 313 K by the method of the substitution titration using MeUmb-Man as a carbohydrate-specific fluorescent indicator. The K_d values at 298.3 K were gradually decreased from MeMan, diMan to triMan (Table 2). These constants were calculated from the fluorescence change and by substitution titration, and the difference was within the experimental error, suggesting the accuracy of the approach on the basis of the fluorescence spectroscopy. The conclusion could also be drawn that mannotriose and its derivatives were the most effective ligands for ConA; their receptor affinities were 1−2 orders higher in comparison with other ligands. In addition, mannotriose did not significantly complicate the drug delivery distinct from complex oligomeric ligands.

Anisotropy (Polarization) of Fluorescence

Fluorescence anisotropy is a rigorous method for studies of interactions of proteins with carbohydrate ligands. The kernel of the method is the polarization of the emission of a fluorescent sample after its excitation with a polarized light. Fluorescence anisotropy characterizes a degree of the sample polarization and is expressed as a difference between parallel and perpendicular components of the fluorescence in terms of the total fluorescence intensity (1) or as the fluorescence intensities at different positions of a polarizer with regard to G-factor (2):

$$r = (I_\parallel - I_\perp)/(I_\parallel + 2I_\perp) \tag{1}$$

$$r = (I_{VV} - G \cdot I_{VH})/(I_{VV} + 2GI_{VH}),$$
$$\text{where } G = I_{HV}/I_{HH}. \tag{2}$$

Several reasons for the depolarization (a decrease in the anisotropy) are known. The main reason is a rotational diffusion of fluorophores. The value of the

fluorescence anisotropy is determined by the rate of rotational diffusion of a fluorophore during the life time of its excited state which, in its turn, depends on the viscosity and temperature of the solution and the volume of the rotating fragment of the macromolecule.

Any external conditions that affect the size, shape, and flexibility of the fluorophore molecule (pH, temperature, viscosity, denaturing under the action of various agents, and others) can influence the fluorescence depolarization. Therefore, the method of the fluorescence polarization is often used for biochemical studies. A measurement of the fluorescence anisotropy is applied to a quantitative evaluation of the dissociation reaction of proteins with ligands [39], and for studies of a complex formation with macromolecules, in particular, for the protein binding to lipid membranes, for the antigen−antibody binding, for protein association, etc. [39−43]. The size, spatial structure, and mobility of segments of a macromolecule are considerably changed during the complex formation, resulting in a change in the observed anisotropy.

The method of fluorescence polarization was used for the determination of the binding parameters of ChitMan5 to ConA (Fig. 6) [34]. Definite excesses of the ChitMan5 ligand were added to the solution of ConA that was covalently bound to the FITC fluorescent label, and the values of the fluorescence polarization were determined. $K_d = 5.5 \times 10^{-5}$ M was calculated from the corresponding absorption isotherm. This value was in a good agreement with the results that were obtained by other methods.

Yuasa et al. [46] applied the method of the fluorescence polarization to a determination of a relationship between the ligand affinity to the lectin and the ligand chain length. K_d of the ConA complexes of oligomannopeptides that contained 1−6 residues of β-aminopropionic acid and one trimannoside per one peptide molecule were determined. The binding efficiency was increased with an increase in the peptide chain length: K_d of the complex proved to be 31×10^{-6} M at $n = 1$, and the minimum value of 9×10^{-6} M was achieved at $n = 3$, i.e., the most stable complex was formed. The opposite effect was observed with the further elongation of the peptide molecule. The stability of the complex was decreased due to the steric factor (12×10^{-6} M at $n = 6$). In addition, these complexes exhibited the higher stability (by one order) in comparison with those with MeMan (Table 2). This fact was explained by the multipoint interactions with the receptor similarly to the chitosan−mannose (ChitMan90). Therefore, the carriers that exhibited such a property are promising for the specific targeting to AM.

Isothermal Titration Calorimetry

The isothermal titration calorimetry (ITC) is a method for determining the thermodynamic parameters of interactions in solution. This method is most
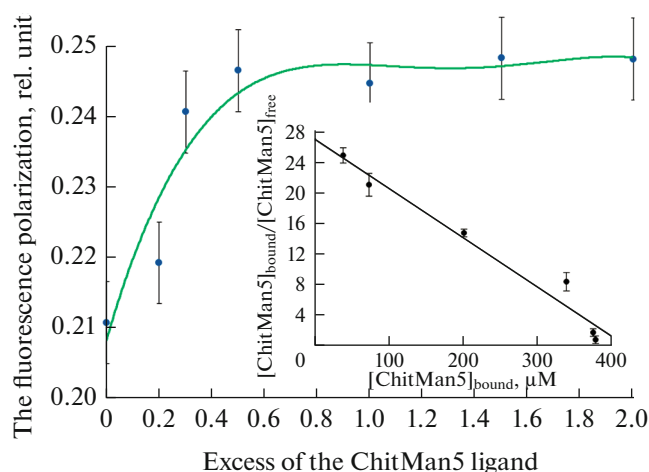

Fig. 6. The dependence of the fluorescence polarization of the FITC-labeled ConA (0.25 mg/mL) on the amount of the added ChitMan5 ligand. The linearization of the sorption isotherm in Scatchard coordinates is shown in the insert [34].

often used for investigation of the binding of small molecules (for example, ligands or medicines) to larger macromolecules (proteins and DNA). A portionwise addition of a ligand to a sample cell during an experiment causes heat absorption or heat liberation. The energy that is necessary for maintenance of equal temperatures of the sample and the reference cell is measured. The enthalpy change, the Gibbs energy, and K_d are calculated from the measurements.

Mandal et al. [47] studied the ConA interaction with various mannose-containing ligands by the ITC method. The dependence of the ligand−lectin affinity on the lectin structure (functional groups and isomerism) was of greatest interest. The K_d values for the ConA complexes with ligands nos. 11−31 are given in Table 2. The following regularities can be revealed on the basis of the calculated energies of the ligand-receptor interactions.

(1) The bond of the C(1) and C(2) atoms of the mannose residues in mannobioses (1,6-; 1,3-; and 1,2) is more effective than that of the C(1) and C(3), C(1) and C(6) atoms. The effect of a fork or an antenna is achieved in the first case (1,2). The binding to the larger number of atoms provides the optimal configuration, and the affinity is much higher where two termini of the ligand participate in the binding. The mannose residues of 1,3- and 1,6-mannobioses are placed far from each other, and no effective binding is formed. The 1,2-isomer is bound three times more effectively.

(2) The analogous tendency is observed for dimannosides (methylated mannobioses). However, the presence of the methyl group in the α-1 position increases the binding efficiency of the 1,2-isomer by 17 times in comparison with 1.6-isomer owing to the

formation of additional hydrogen bonds and the absence of steric hindrance.

(3) No significant differences in the affinity is found for trimannosides and mannotrioses, because the ligand contains three mannose residues which are effectively bound in the 1,6-, 1,3- and 1,2-isomers. The further addition of the mannose residues cannot result in the binding improvement due to the steric hindrance. However, the addition of the terminal *N*-acetylglucosamine residues to 3,6-di-*O*-(mannopyranosyl)-α-mannopyranose increases the efficiency by 4.2 times. Ligand 27 (Table 2) proves to be the most specific to ConA among all the presented ligands.

(4) The tendency to an increase in the ConA affinity is observed when passing from monomannosides to dimannosides and trimannosides owing to an increase in the number of atoms that form bonds without spatial hindrances.

(5) The presence of symmetrical (identical) termini of the glycopeptide ligand as bi-antennas and tri-antennas increases the binding efficiency: K_d of Man9 differs from those of Man7 and Man8 by 3.6 times. As a rule, different unsymmetrical groups decrease the interaction strength with the receptor, because steric hindrances decrease the number of hydrogen bonds.

(6) Methylation of the OH-groups of the C(6) atoms of carbohydrates strongly enhances the affinity to the lectin. The efficiency increases by 2.9 times for mannose, 3.4 times for dimannose, and 1.5 times for trimannose.

(7) Thus, the use of the triantenna ligand and symmetrical *N*-acetylglucosamine termini improves the specificity of the ligand−receptor interaction by several orders. K_d of the ConA complexes is 122 μM for Man and 0.71 for 3,6-di-*O*-(β(1,2)-GlcNAc-mannopyranosyl)-α-mannopyranose (15 and 27 in Table 2, respectively). The binding efficiency increases 172 times, i.e., by two orders.

Dam et al. [48] implemented the idea of the creation of the multivalent ligand. They synthesized trivalent and tetravalent derivatives of trimannoside (nos. 32 and 33 in Table 2). These compounds formed vary stable complexes with ConA (K_d was approximately $10^{-7}-10^{-8}$ M).

As follows from the experimental data (see Table 2), the ligand affinity to the receptor increases with the enhancement of the content of the available Man residues. Trimannosides more effectively recognize ConA than monosaccharides and disaccharides. Moreover, an additional improvement of the binding efficiency is achieved by the introduction of the terminal acetylglucosamine residues (GlcNAc).

The aforementioned tendencies are explained by differences in the *N*-glycosylation processes and structures of the cell walls of bacteria and eukaryotes (oligosaccharide antigens and exposed carbohydrate residues). MRs of macrophages and DCs serve for recognition of prokaryotic organisms and fungi, thus, MRs mediate the pathogen killing and support the inborn and adapted immunity. The CD206 receptor binds the "open" residues of D-mannose, *N*-acetylglucosamine, and fucose of glycans on a surface of the pathogenic microorganisms, for example, mycobacteria whose cellular wall consists of the cross-bound peptidoglycans (murein), lipoarabinomannan, a layer of complex polysaccharides (arabinogalactans), surface mycolic acids, and a layer of external glycolipids, which are responsible for the high bacterial resistance. Note that the cells of yeast, plants, and insects also have the large number of available Man residues in the lipid-bound oligosaccharides. These Man residues are only partially "closed" with fucose and galactose in plants. However, animals (except mammals) have a "protection" that consists of galactose and *N*-glycolylneuraminic acid, and mammals are additionally "protected" by Neu5Ac [49].

Thus, the multivalent oligosaccharides from the Man and GlcNAc residues are the most promising for the effective binding to the mannose receptors (for example, nos. 25−33 in Table 2). The revealed regularities allow a synthesis of the ligand that will be highly specific to ConA and, hence, to MRs for an elaboration of the optimal carrier for medicines.

Lectin Affinity Chromatography

Lectin chromatography is a form of affinity chromatography in which lectins are used for fractionation of the carbohydrate-containing components of a sample. A lectin which is immobilized on an insoluble matrix (for example, on an agarose base) serves as a stationary phase. The mixture is fractionated in the mobile phase via selective binding of the carbohydrate-containing ligands [50, 51]. The widespread carriers for the lectin affinity chromatography are ConA-sepharose and sepharose-immobilized agglutinin of the wheat germs that binds *N*-acetylglucosamin. The most-used application is a separation of glycoproteins from nonglycosylated proteins [52, 53]. The biospecificity is determined by a conformational correspondence between ligands and receptor binding sites [54].

Le-Deygen et al. [34] examined the stability of the ConA−ChitMan5 complex by this method using ConA-sepharose as a carrier. ChitMan5 was applied onto a column with ConA-sepharose, and the column was eluted with a gradient of mannose (0.1−1.0 mM). Most of the complex was found to be decomposed with a 7.5-fold excess of mannose; hence K_d of the ConA−ChitMan5 complex was ~7.5 times lower than that with mannose. This fact was in a good agreement with the calculated K_d of the complexes; the K_d values were differed by ~7 times (Table 2). Therefore, parameters of the ligand−protein binding could be determined by affinity chromatography relatively to an

etalon, and one could also prove that a ligand specifically interacted with ConA precisely in the mannose binding site.

The method of lectin chromatography is used for a preparative isolation of lectins from cells. Argayosa et al. [55] reported an isolation of the mannose-binding lectin (MBL) from a serum of the African sheatfish. An affinity column with mannan–agarose was used for purification of the protein. The isolation of this lectin stimulated an investigation of interactions with pathogens that expressed the mannose ligands. Components of the cellular wall of the *C. albicans* pathogenic yeasts that contained β-1,2-bound oligomannosides and phosphomannan from the cellular wall of the *S. cerevisiae* were potential target ligands for the mannose-binding lectin. The bacterial cells with lipopolysaccharides which contained many terminal mannose residues (ManNAcUA-GlcNAc and GlcManNAcUA-GlcNAc) were also effectively recognized by MBL.

Pawley [56] applied affinity chromatography to isolation and identification of rice proteins. The rice extracts were fractionated by column affinity chromatography using mannose as a ligand. The bound fractions were eluted and subjected to electrophoresis and HPLC. One hundred and thirty-six various mannose-binding proteins were obtained from rice. A comparative analysis demonstrated very little overlapping of the identified proteins between the corresponding tissues. Almost 15% of the proteins were not described before, pointing to an importance of this chromatographic method for lectin isolation, including the mannose-binding lectins, and studies of their properties.

Confocal Microscopy

Confocal or laser scanning microscopy (CLSM) is widely used for a visualization of biological objects at a submicron scale, including AMs which interact with medicamentous molecules in nanoparticles [57, 58]. The "capture" of two-dimensional images at different depths in the sample allows a reconstruction of three-dimensional structures inside the object.

Ghotbi et al. [59] studied the binding and the absorption efficiency of the mannan-decorated nanoparticles from the lactide–glycolide copolymer by the dendritic cells (DCs). The DC suspensions were stained by the FITC-labeled CD11c (the integrin that induced the cellular activation and the synthesis of the reactive oxygen species for a fight against pathogens). The nuclei were stained with diamino-2-phenylindole. The fluorescent staining of parts of the cells demonstrated that the dendritic cells expressed the mannose receptors and CD11c similarly to macrophages. In addition, the interaction of the different mannan-decorated nanoparticles (the carriers with the absorbed mannan or the mannan that was chemically bound to DCs were taken) was examined by

CLSM (Fig. 7). Singular cellular images of the fixed cells confirmed the effective intracellular absorption of the mannan-modified particles, rather than weak binding to the DC surface as observed in the case of the nonmannosylated nanoparticles. The presence of the point red spots in the cytoplasm affirmed this fact. All the types of modified particles penetrated into DCs, but the particles with the covalently-bound mannan proved to be the most effective (Fig. 7c).

Chen et al. [60] determined absorption of various nanoparticles by the J774E MR-expressing cells of the mouse macrophages by CLSM using the fluorescent labels (FITC and 4',6-diamino-2-phenylindole). The spacer length, the distance between the mannose residues, and the molecular mass of the polymer were varied. The optimal parameters of the carrier at which the absorption by the target cells was the most effective were determined on the basis of the data obtained. Figure 8 illustrates an influence of the number of the mannose residues per one nanocapsule and the distance between the mannose residues on the cellular absorption of the modified carriers. The particles in which two mannose residues were at a distance of 56 Å from each other (this distance was close to that between the ConA binding sites) proved to be optimal.

Thus, confocal microscopy with the application of fluorescent labels allows an investigation of a relationship between various parameters of the drug carrier (size, molecular mass, modification degree, and distance between the mannose residues) and its absorption by the target cells (MPhs and DCs).

Flow Cytometry

Flow cytometry (FC) is a highly informative method for studies of cells in dispersion media in a regime of single analysis of elements by means of light dispersion and fluorescence. Cells are evenly passed through a center of focused laser beams in a flow cytometer for an exact measurement of the cellular optical properties [61, 62]. The FC results can be imaged as histogram or two-dimensional or three-dimensional point diagrams. Areas on these regions can be subsequently divided on the basis of the fluorescence intensity. Several areas that characterize an expression of definite antigens can be separated. The fluorescence diagram is analyzed as follows: the fluorescence values of two fluorophores that are proportional to the number of cells with the analyzed antigens of the surface ligands are plotted on the axes, respectively, and an expression of molecules in the examined sample is determined [63].

Ying et al. [64] have used FC for determination of the surface expression of antigens and the mannose receptors (CD11b, F4/80, CD11c, CD206, CD69, CD80, and CD86) which were responsible for the recognition of the mannose ligands on MPhs. The authors have also studied changes in the phenotype of
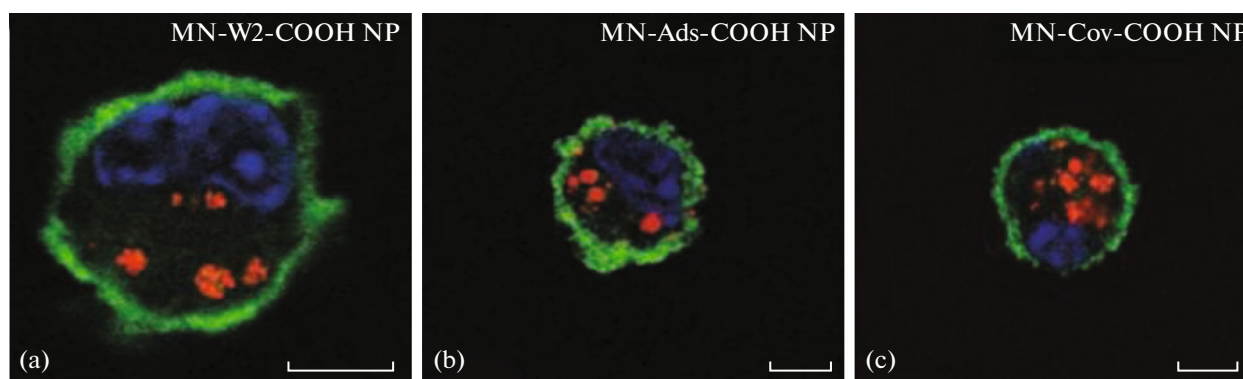
Fig. 7. A visualization of the absorption of particles by the dendritic cells with the use of the confocal microscopy: (a) MN-W2-COOH NPs; (b) MN-Ads-COOH NPs; (c) MN-Cov-COOH NPs, (MN, mannan; W2, emulsification; Ads, adsorbed; Cov, chemical binding; NP, nanoparticle). The red points inside the cells indicate the localization of the TMRD-loaded nanoparticles in a cytoplasm. The scale interval is 5 μm [59].
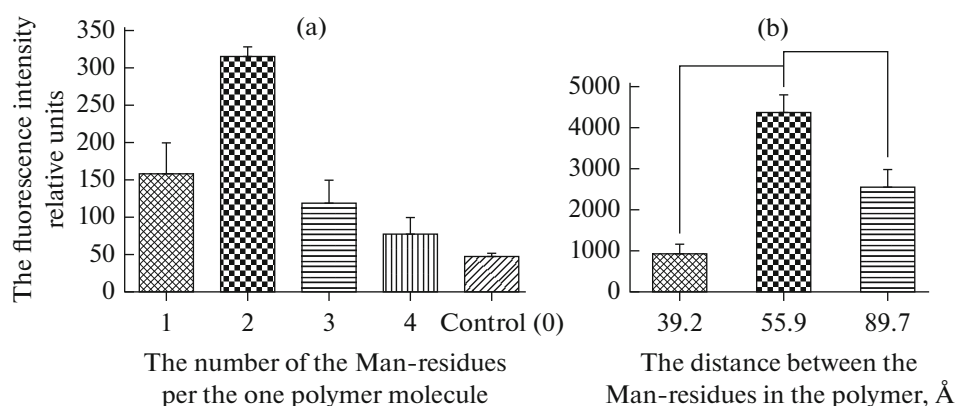

Fig. 8. The fluorescence intensity (the relative units) as an indicator of the cellular absorption of the drug carriers depending on (a) the number of the mannose residues per one polymer molecule and (b) the distance between the mannose residues [60].

macrophages during their activation by FC. Two variations of the MPh activation have been considered: the classic activation (the M1 immunoactive) and the alternative activation (the M2 opposite). As discussed above, the MPhs are activated under the action of signal substances which were produced in response to an exposure to negative factors, for example, viruses or bacteria. M1 depends on the Toll-like receptors (TLRs) and the activation of the nuclear factor that induces production of such cytokines as TNF-α and IL-1β, resulting in an enhanced release of the reactive oxygen species, for example NO [65, 66]. Therefore, immune-activating M1 MPhs kill viruses and bacteria. On the contrary, the M2 activation of macrophages (under the action of the IL-4, IL-10, or IL-13 cytokines) results in an increase in the expression of CD206 MR and arginase. The M2 MPhs produce polyamines (in order to induce proliferation) or proline for the collagen synthesis. These MPhs are associated with wound healing and tissue reparation. The anti-inflammatory MPhs are activated in the M1 direction during the early phase of the *Mycobacterium tuberculosis* infection. Further, MPhs acquire predominantly the M2 phenotype in order to preserve the tissue homeostasis of lungs and avoid the cytokine storm.

The addressed targeting to AMs can be used in several cases. First, mycobacteria penetrate inside MPhs, gain protection, and block the immune-activating function of AMs during severe disease. In this case, delivery of antibacterial agents (for example, rifampicin) is necessary for killing the pathogen because the immune system cannot overcome the disease. Second, the normal quantities of the M1 and M2 activated MPhs exist. Both excess and deficiency of the definite AM phenotype result in disorders of the functioning of the immune system. The level of the M1 and M2 activation can be stabilized by a treatment with therapeutic agents, for example γ-interferons, interleukins, methyl uracil, the bacteria-imitating lipopolysaccharides or, on the contrary, by an administration of inhibitors of the T-lymphocyte functions, blockers of the IL-33 receptors, or the interferon neutralizers.
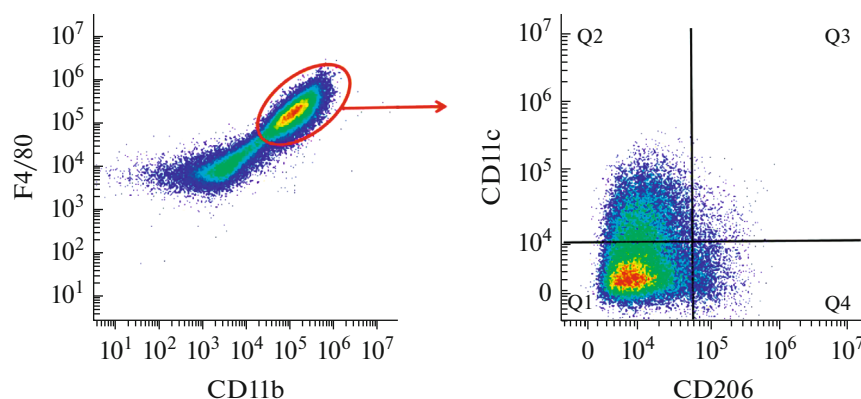
Fig. 9. An analysis of macrophages by flow cytometry. The number of the fluorescent cells is plotted along the axes. All the examined macrophages express the CD11b integrin and the F4/80 antigen. The $CD11b^+F4/80^+CD11c^+CD206^-$ phenotype is found for the M1 MPhs, corresponding to the Q_2 area, whereas the M2 MPhs are the cells with the $CD11b^+F4/80^+CD11c^-CD206^+$ phenotype (the Q_4 area) [64].

Ying et al. [64] investigated the MPh activation through the M1 and M2 paths. The L-929 macrophages that were widely used as the in vitro model were obtained from mouse bone marrow. The M1 and M2 activations were stimulated by lipopolysaccharides and by IL-4 and IL-13, respectively. The FC method demonstrated that the MPh activation via both pathways resulted in an augmentation of the MPh size and increase in the expression level of antigens and proteins on the cellular surface (CD206, CD69, CD80, and CD86) (Fig. 9). In the case of M2, the level of expression of CD206 and the above mentioned antigens was enhanced by 3−5 times, whereas MI caused an even higher increase by 10−50 times. Thus, the changes that occurred in MPhs during their activation were revealed, and the biomarkers for both MPh phenotypes were determined by FC.

In addition, the FC method allows a determination of the phenotype of MPhs and DCs [67]. The MPh receptors were examined using neoglycoconjugates in which a carbohydrate is attached to the fluorescein-labeled polyacrylamide. The synthesized ligands were bound to MPhs from the blood of healthy donors. An expression of the CD11c, CD14, CD36, and CD40 on MPhs was determined according to a change in the fluorescence intensity by FC. The CD83, CD86, and CD15 that were characteristic of the dendritic cells were not found on the MPh surface. These results exactly pointed to macrophages and the state of their activation in vivo (because other ways of the MPh activation can exist and can be identified from the MPh phenotype). Moreover, possibilities of a targeting to these MPh antigens and a regulation of the MPh activation are opened up.

Another example of the FC application to the phagocytosis investigation is a study of the role of the MPh lectins, in particular, Siglecs (the sialosid-binding lectins), in elimination of the apoptotic bodies as one of the important macrophage functions [67]. Studies of the phagocytosis process, in particular the receptors that are responsible for a primary recognition, give possibilities for a directed stimulation of phagocytosis at early stages of oncogenesis. Lectins participate in phagocytosis through a binding to the complementary carbohydrates of the target cells. Neutrophils first penetrate into a cancer and, then, attract the secondary effector cells (macrophages and cytotoxic T-lymphocytes) to this cancer. These cells secrete products that can activate neutrophils and their anticancer activity. MPhs and immature DCs also can absorb cancer cells. Therefore, a stimulation of the neutrophil penetration into the cancer tissues can be a promising method for a treatment of oncological diseases.

The sialosid-binding lectins (siglecs), such as siglec 1, 5, 10, 11, and 15, are expressed on macrophages and can be used as a target for an immunotherapy [68−70]. Siglecs are exposed on the immune and blood cells, recognize chains of glycoproteins and glycolipids of a cellular membrane, and participate in pathogen recognition. Rapoport et al. [67] performed FC analysis of the interaction of macrophage from the blood of a healthy donor and a patient who suffered from breast cancer and found that the cells involved the siglec which interacted with the Neu5Aca(2−3)Gal-containing and Neu5Ac-α(2−6)Gal-containing glycans, and an expression of this siglec was increased during the disease. However, siglec1 and siglec5 exhibited the highest affinity to Neu5Ac-αOBn. A conclusion was drawn on the basis of the change in the lectin expression that they play a key role in the MPh and DC recognition and the subsequent elimination of the apoptotic bodies.

*X-ray Analysis (XRA) of the Complexes of Lectins
with the Mannose Ligands: Neutron Crystallography*

Crystallographic methods are effective for the studies of structures of the protein–ligand complexes. Naismith et al. [36] studied the interaction of ConA with 3,6-di-*O*-(mannopyranosyl)-α-mannopyranose (hereinafter referred to as trimannoside) by XRA of a monocrystal of the lectin–ligand complex with a resolution of 2.3 Å. The authors identified the sites that were responsible for the binding. 1,6-Terminal mannose (O3, 4, 5, and O6 were most involved) was bound to Tyr12, Asn14, Gly98, Leu99, Tyr100, Ala207, Asp208, Gly227, and Arg228. The reducing carbohydrate (O2, 4) was bound to Tyr12, Asp16, Leu99, and Arg228. The 1,3-terminal mannose (O3, 4) interacted with Tyr12, Pro12, Asn14, Thr15, and Asp16 (Fig. 10a). In addition, the distances between the interacting atoms were determined (2.5–3.5 Å, 3 Å in average). The O6 atoms proved to be effectively involved in the binding to the lectins which consisted of several mannose residues. Thus, the affinity of dimannoside to the 1,6-bond was decreased, because the O6 atom could not interact with ConA, and the constant values confirmed this fact (Table 2).

Gerlits [37] determined in more detail how the interaction of the ConA with mannobiose occurs by neutron crystallography (Fig. 10b). The tetrameric lectin binds mannobiose on a region of the protein surface (12–16, 98–100, 207, 208, and 226–228 amino acid residues), and these results were in a good agreement with the data of Naismith et al. [36]. The unreducing (terminal) mannose residue (Man1) formed six direct hydrogen bonds and one water-mediated interaction with ConA, whereas the reducing mannose residue (Man2) had only one direct hydrogen bond and one water-mediated contact. The disaccharide had an advantage over monosaccharides owing to the additional interactions. Man1 O3 formed the hydrogen bond with the carboxyl group of Asp71, and Man2 O1 had the strong hydrogen bond with the main chain of the Ser184 carbonyl. The mannobiose binding did not significantly change the carbohydrate-binding site of ConA, but the Asp16 and Leu99 atoms of the main chain were considerably affected. Both of them were shifted by ~1 Å in the direction of the disaccharide with the formation of hydrogen bonds and hydrophobic interactions with the ligand. Only positions of side chains of other residues were changed. For example, Tyr100 and Arg228 in the ConA–mannobiose complex were shifted from their corresponding position in the ConA structure in order to prevent the steric hindrances. Thus, the ConA binding site was already preliminarily formed before the disaccharide binding. The ligand binding induced small alterations in the positions of the side chains of the proximal amino acid residues.

XRA demonstrates that, in a number of cases, two variations of the lectin binding to a ligand occur [71].

Such bindings are shown by the examples of structures of the ERGIC-53 and VIP36 mannose-specific lectins of the L type which contain the ConA-like carbohydrate recognition domains (CRDs). The carbohydrate-binding site of ERGIC-53 also requires the presence of the Ca^{2+} ions. The Man-α(1,2)-Man ligands are identified according to a change in the electron density in the four CRD sites. Site 3 interacts with Asp121 (O1 and O2), Asn156 (N2), Gly251 (N), Gly252 (N), and Leu253 (N) via hydrogen bonds in the complex. Phe154 is involved in the hydrophobic interaction with the C4, C5, and C6 atoms of this mannose residue. The mannose residue of site 2 forms a hydrogen bond between 4-OH group and Ser88. Two alternative ways of the Man-α(1,2)-Man accommodation in the CRD carbohydrate-binding site of ERGIC-53 are possible: sites 1, 2, and 3 are involved according to the first way (regime I), whereas sites 2, 3, and 4 participate in the second way (regime II) (Fig. 11). The same variations exist for ConA. The 3-OH group of Man (D1) is placed outside the carbohydrate-binding pocket (regime I), and the Glc-α(1–3)-Man bond is formed without any steric hindrances. However, this binding regime is not characteristic of CRD VIP36, because the Man(4) reducing mannose residue intensively interacts with Tyr164 in site 4, and regime II dominates. In this regime, the Man residue (D1) is placed in site 2 of ERGIC-53 in the direction of the loop that involves Gly251, Gly252, and Leu253 due to the absence of the bulky side chain of aspartate. Such a structural position provides the carbohydrate recognition by ERGIC-53-CRD without steric hindrances. Two binding ways are also typical for ConA, but the second way is predominant [72].

Moothoo et al. [72] have discussed the recognition ways of the ConA mannose residues. The reducing terminal carbohydrate of subunit A is recognized by the monosaccharide site via a combination of hydrogen bonds, polar contacts, and Van der Waals interactions similarly to that for methyl-α-D-mannopyranoside. A shift of the position of the mannose ring by 0.3 Å from the binding place is observed. The unreducing residue occupied the new place, and the main conformation was formed. On the contrary, the unreducing terminal mannose residue of subunit D is located in the monosaccharide site and interacts with Gly98, Ser168, and Thr226. The reducing residue takes the other conformation relatively to the glycoside bond in order that the methyl group can penetrate into the hydrophobic pocket. The electron density appropriate for both binding ways is observed for the third subunit, and both variations occur. The binding regime in subunit A is impossible for subunit D owing to small structural differences of the sites. Although the amino acid sequences of all the four subunits of ConA are identical, small differences exist in their structural organization (the relative location of the chains), resulting in the above-discussed peculiarities.
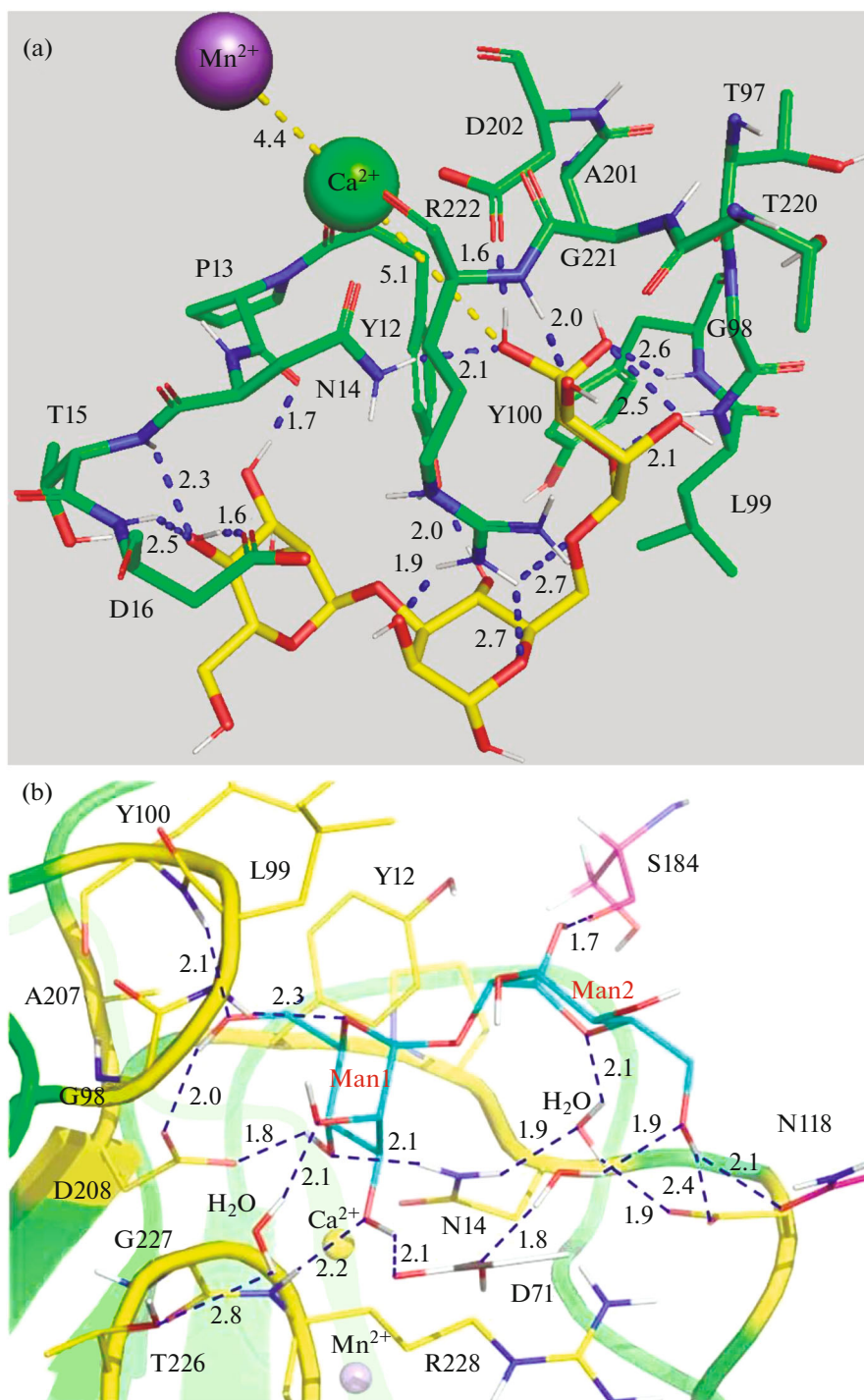
Fig. 10. (a) The interaction of ConA and 3,6-di-*O*-(mannopyranosyl)-α-mannopyranose (trimannoside). The green and yellow colors correspond to the receptor and the ligand, respectively. The green and violet spheres are Ca^{2+} and Mn^{2+}, respectively. The one-letter indexes of the residues are given. The distances are expressed in Å. PDB: 1ONA; (b) the interaction of ConA with dimannose (according to X-ray analysis). The yellow and blue colors correspond to the receptor and the ligand, respectively. The distances are expressed in Å [37].

Thus, the crystallographic methods allow studies of the protein−ligand interaction at the atom−molecular level, reveal the common lectin motifs for carbohydrate recognition, and obtain data on the structural organization of the complexes for computer modeling.

Combination of Various Methods for a Determination of the Ligand−Receptor Binding Parameters

Several methods are used for a complete and detailed analysis of the protein−ligand interactions.
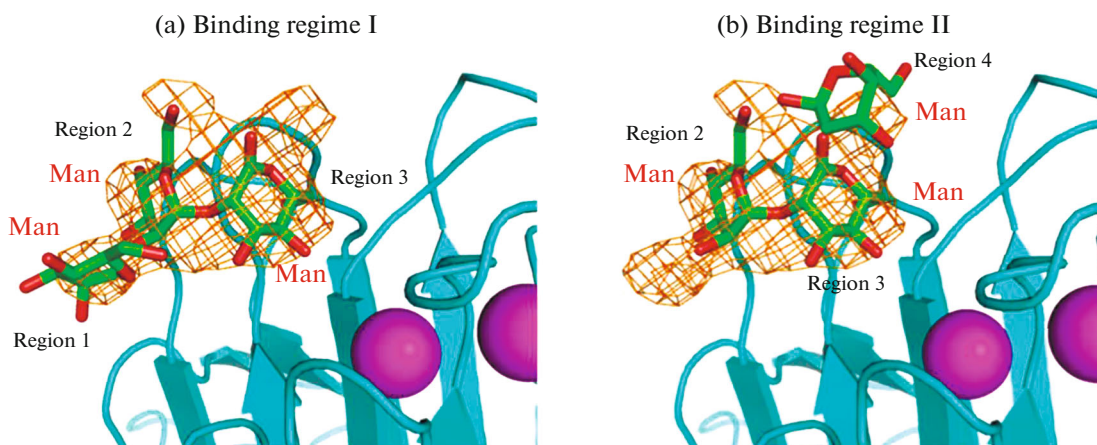
(a) Binding regime I

(b) Binding regime II

Fig. 11. Regimes (a) I and (b) II of the binding of the ERGIC53 lectin to the mannose-containing ligand [71].

Such an approach allows an increase in the data adequacy and determination of the binding parameters. We will discuss the investigation in which confocal microscopy and flow cytometry are used for an analysis of the absorption of a drug carrier and spectral fluorescence for a confirmation of the addressed delivery. Freichels et al. [73] studied the binding of the mannose ligands (mannose, dimannosides, and trimannosides) that were immobilized on nanocapsules (NCs) from the covalently bound hydroxyethylstarch and polyurethane to the model ConA receptor and DCs by the fluorescence methods, flow cytometry, quantitative NMR, and confocal microscopy. The ability of the mannose-functionalized NCs to interact with the FITC-labeled *Galanthus nivalis* agglutinin was examined depending on the type of mannose ligand, the density of the mannose residues per one surface unit, and the presence of the PEG linker. The interaction of these mannosylated NCs with the fluorescent lectin demonstrated a steric availability of mannose during the binding to the model ConA receptor. The best binding was observed for diMan and triMan which were placed on the NC surface owing to the high affinity of the lectin to these carbohydrates in comparison with mannose (Table 2). The introduction of the PEG linker between NCs and the carbohydrate resulted in an increase in the interaction with the receptor that was mainly associated with the better availability of Man. The quantitative parameters of the carriers were determined by ^{13}C NMR. The optimal surface density of the ligands proved to be 0.13 units/nm^2. This value was equivalent to 26 000 of the mannose ligands per one nanocapsule.

The target function of the mannosylated NCs were demonstrated for DCs. Absorption of NCs by the dendritic cells was grown by ~3 orders due to the binding of the cellular receptors to mannose on a surface of these capsules. This binding was demonstrated by FC with the use of the FITC-labeled NCs. Confocal laser scanning microscopy showed that the unmodified NCs were mainly nonspecifically absorbed on the cells, whereas the mannosylated triMan NCs were more effectively absorbed by the target cells. However, the differences in the binding efficiency of the mannosylated carriers were weak (<2 times), therefore, all the examined nanocapsules could be considered as effective.

Thus, the results of the above-described experiments suggest that the interactions of ConA, MPhs, and DCs with the mannose receptors are similar. The same tendencies are observed: an increase in the number of the mannose residues in a ligand results in an improvement of the efficiency of the ligand–receptor binding, and the presence of spacers in a carrier is necessary. The in vitro experiments with the model proteins are required for a determination of the most affinity ligands with regard to the optimal degree of mannosylation, the optimal molecular mass of a molecule, and the presence and nature of a spacer. Biosafety, biodegradation, and the specific interaction of the selected conjugates with the target receptors of cells (MPhs) are further examined.

CREATION OF THE MANNOSYLATED CARRIERS FOR THERAPEUTIC AGENTS WITH THE ADDRESSED DELIVERY FUNCTION

The glycosylated polymeric carriers (conjugates of such natural polymers as chitosan, dextrins, liposomes, PEG with carbohydrate fragments, including mannose, galactose and others) are successfully used for a delivery of different therapeutic agents, including antiviral drugs (azidothimidine and stavudine), antitumor medicines (methotrexate and doxorubicine), antituberculous drugs (rifampicin), antigens (the surface antigen of the hepatitis B virus), and others [74]. A promising approach is the creation of carriers for antituberculous drugs (ATDs) that are targeted to the mannose receptors of the alveolar macrophages. A

high efficiency of the AND delivery to the macrophages with the use of the Man-containing carriers has been demonstrated in the in vitro experiments. Methods for a synthesis of complexes and conjugates of various carriers (polymers, liposomes, and lipid particles) with mannose are well-proved. One can prepare particles of the desired composition, size, and modification degree. Favorable in vivo effects are found for the ATD-loaded mannosylated carriers (liposomes, solid lipid particles, and chitosan), in particular, an enhancement of the basic and maximum ATD concentration in lungs, a decrease in the ATD concentration in the blood plasma (an alleviation of the toxic effects of medicines), and the absence of the hepatic toxicity. Below, we will discuss examples of the created systems of the addressed delivery of drugs and their efficiency.

Liposomes: Lipid Particles

An application of the mannosylated liposomes to the ATD delivery is reasonable and effective for an enhancement of the basic and maximum concentration of ATDs in lungs. Garg et al. [75] demonstrated that the liposome glycosylation increased the degree of absorption of azidothimidine (the antiviral drug, the nucleoside inhibitor of the reversed transcriptase of the human immunodeficiency virus) by the alveolar macrophages in 8.5 times in comparison with unmodified carriers.

Chono et al. [76] obtained similar results in the course of their studies of a relationship between the mannosylation degree of liposomes and their absorption by AMs. 4-Aminophenyl-α-D-mannopyranoside was used for the modification, and the liposomes (the particle size was 1 μm) with different mannosylation degree were prepared. The AM absorption of the liposomes in the in vitro experiments was increased with an increase in the mannosylation degree within the range from 2.4 to 9.1 molar Man % and was not further changed. The mannosylated liposomes (9.1% Man) were more effectively delivered to AMs in the in vivo experiments after the lung aerosolization of rats in comparison with the unmodified liposomes (24 and 13%, respectively). The NR8383 cells absorbed the mannosylated liposomes by endocytosis which was mediated by the mannose receptors. This process was demonstrated in the experiment of the competitive binding in the presence of mannose [76]. Thus, the liposome modification with mannose was shown to be effective for the addressed targeting to MR of macrophages.

Kawakami et al. [77] and Wijagkanalan et al. [78] proposed a promising method for the liposome modification during studies of the intratracheal administration of the mannosylated liposomes (Man-liposomes) with a different ratio of the mannosylated cholesterol derivatives (Man-C4-Chol) to mice. The chemical structure and physicochemical characteristics of Man-C4-Chol met the conditions of a transfection into MPhs. Man-C4-Chol were positively charged and were effectively recognized by the mannose receptors. Man-C4-Chol derivatives were shown to exhibit a high transfection activity. The cells absorbed the Man-liposomes with the 7.5 and 5% content of Man-C4-Chol ~3 times more effectively than those with 2.5% and zero content of Man-C4-Chol. In addition, the Man-liposome absorption was significantly inhibited by the mannose excess, suggesting mannose-receptor-mediated endocytosis [77, 78]. The high internalization efficiency and the selective targeting to AMs were observed in the in vivo systems after the intratracheal administration of the highly-mannosylated liposomes (7.5%) to rats.

Solid lipid nanoparticles (SLNs) are used as lipid carriers of medicines along with liposomes. The SLN absorption by cells can be increased due to the SLN larger size (200–500 nm). However, solid lipid nanoparticles are generally used for the water-insoluble drugs, whereas liposomes are more universal. Nimje et al. [79] studied possibilities of the SLN application to the selective delivery of the rifabutin antituberculous drug in the alveolar tissues. Solid lipid nanoparticles (M-SLN-R) were synthesized, loaded with rifabutin (R), and mannosylated. Absorption of these particles by macrophages was determined on the basis of the particle fluorescence [79]. The SLN mannosylation increased absorption by the cells 5.8 times. The similar picture was also observed in the in vivo experiments. The use of the mannosylated liposomes increased the time of rifabutin circulation in rat blood from 48 to 72 h for SLN-R (the unmodified particles) and from 48 to 96 h for M-SLN-R. The predominant absorption of M-SLN-R by the alveolar macrophages was observed. Such a specific absorption facilitated the selective penetration of the particles into lungs and prevented their entry to other organs. The increase in the average size of the particles from 251 to 389 nm after the mannosylation of the lipid nanoparticles was observed using scanning electron microscopy. This increase was also the efficiency factor. The larger particles (M-SLN-R, in this case) were predominantly absorbed by macrophages distinct from small particles.

Thus, the liposomes that are conjugated with the mannose ligands can be used for the effective targeted delivery of therapeutic agents and can finally reduce their side effects.

Polysaccharides: Chitosan and Mannan

Polysaccharides (such as mannan, chitosan, and others) are promising carriers of medicines. Their special characteristics are availability, biocompatibility, mucoadhesiveness, and the absence of a negative effect on metabolism. Mannan is a plant polysaccharide, a linear polymer that is formed from the $\beta(1-4)$-connected mannose residues. Mannan from the yeast cellular wall is also known. This mannan involves the

Table 3. The physicochemical properties of nanoparticles of the mannosylated chitosan with oligodeoxyribonucleotides determined by photon correlation spectroscopy [83]

ChitMan/ODN ratio	Particle size, nm	ζ-Potential, mV	The number of ODNs, which were absorbed by 1 million of the cells, ng
1 : 1	267.12 ± 11.0	−6.2 ± 0.02	30
3 : 1	192.48 ± 4.8	+8.9 ± 0.82	74
5 : 1	187.16 ± 5.6	+12.6 ± 0.64	65
7 : 1	178.24 ± 7.4	+14.2 ± 0.46	60

main chain with the $\alpha(1-6)$-bonds and side chains in which mannose are connected by $(1-2)$-bonds and $\alpha(1-3)$-bonds.

Chitosan is an amino polysaccharide whose molecules consist of deacetylated (by 70−90%) units of β-(1−4) *N*-acetyl-D-glucosamine. An application of chitosan as the ATD carrier is associated with its ability to decrease the toxicity of antibacterial agents and to enhance absorption of the ATD-loaded particles by macrophages [80]. The chitosan is mannosylated by a reaction of the chitosan amino groups with mannose or its derivatives. Three types of functional groups that are available for a modification are present in the chitosan molecule: the primary amino groups and the primary and secondary hydroxyl groups. The easiest way to prepare the mannosylated chitosan is a direct reaction of chitosan with α-D-mannose. The binding degree of chitosan to lectin can be increased by the chitosan glycosylation by the Maillard reaction (it is a chemical reaction of the reducing sugars with amino acids) or by the use of a condensing agent (for example, by the active ester method) [81, 82].

Asthana et al. [83] prepared the mannosylated chitosan nanoconstructs (22 kDa, the deacetylation degree of 72.5%) for a delivery of oligodeoxyribonucleotides (ODN) into MPhs. The mannosylated water-soluble chitosan demonstrated a good ability for the receptor binding (the RAW 264.7 mouse macrophages were used) and optimal physicochemical properties (the particle size and the ζ-potential) (Table 3). The transfection efficiency depended on the ChitMan/ODN ratio. A significant increase in the transfection efficiency was observed with the increase in the ChitMan/ODN ratio from 1 : 1 to 3 : 1. The latter ChitMan/ODN ratio was optimal. ChitMan-ODN exhibited the higher transfection efficiency (by ~3 times) under these conditions in comparison with the free ODN. The free mannose competed for the binding sites with the receptors. As a result, the transfection efficiency of ChitMan-ODN was decreased with an increase in the mannose concentration and absorption of the nanoparticles was inhibited by ~50% at the mannose concentration of 20 mM. Therefore, the penetration process of the mannosylated macromolecule into macrophages through the mannose-receptor-mediated delivery system was confirmed again.

Budzynska et al. [84] demonstrated an enhancement of the transfection efficiency of an antitumor agent after its conjugation with mannan (mannan is a polysaccharide that is isolated from the *Saccharomyces cerevisiae* yeasts). The mannan−methotrexate conjugate exhibited improved antitumor activity in the in vivo experiments in comparison with the free medicine on the model of the P388 mouse leucosis in the abdominal cavity.

Thus, the mannosylated polysaccharides (chitosan and mannan) are effectively absorbed by macrophages and are biosafe and biodegraded carriers for therapeutic agents.

Dendrimers

Dendrimers are promising carriers for drug delivery (for example, antitumor agents) along with the aforementioned polymers. Dendrimers are repetitive branched molecules. The dendrimers of several generations are distinguished according to the number of branchpoints. The dendrimers of the third generation are characterized by the high density of their molecular structure and an almost spherical shape. Their solutions have much lower viscosity than those of other substances with the same molecular mass. Physical characteristics of dendrimers are monodispersivity, water solubility, ability for encapsulation, and the large number of functionalized peripheral groups. These properties stimulate the dendrimer application as addressed agents for drug delivery. Dendrimers are universal as objects for a wide spectrum of chemical modifications which can be performed for an enhancement of biocompatibility and other characteristics.

Biodistribution and cellular absorption of the synthesized delivery systems (dendrimers) were investigated using rabbit and mouse cellular lines [85]. The dendrimers of the fourth generation on the basis of polyamidoamine (analog, Fig. 12) were modified with mannose for a targeting to the mannose receptors. The efficiency of cellular absorption was evaluated on the RAW 264.7 mouse cell line by fluorescence microscopy. The absorption increase by 2.5 times was shown
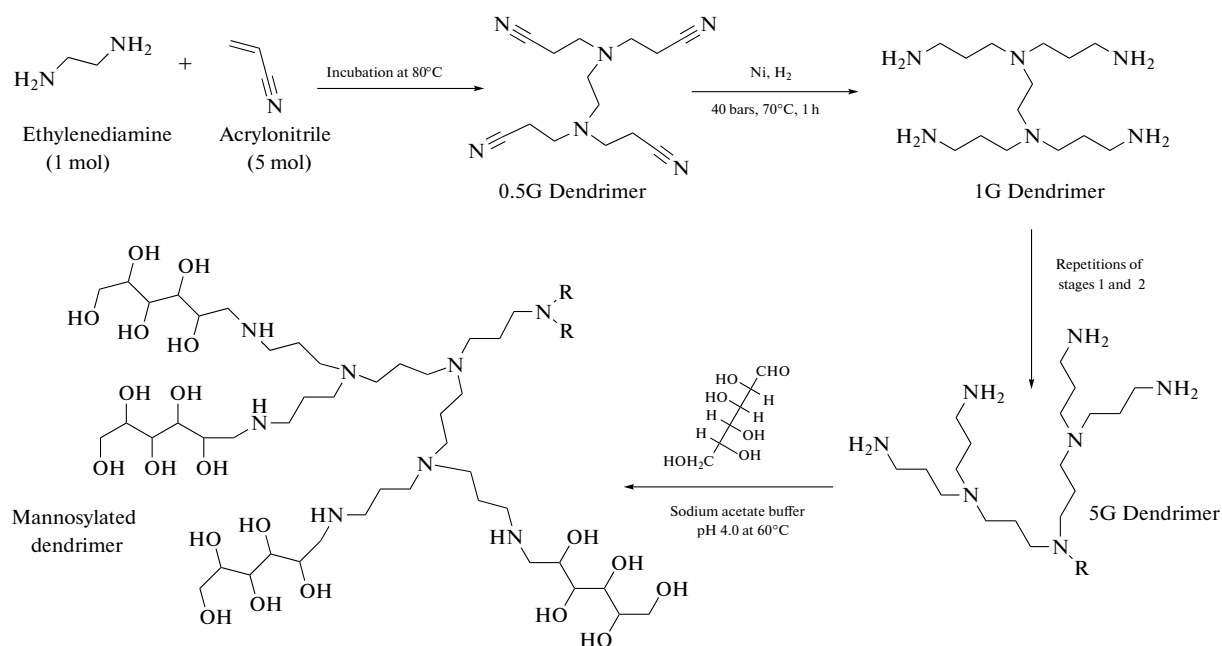
Fig. 12. The synthetic scheme of the mannosylated dendrimer of the fourth generation [87].

in comparison with the unmodified ligands. The in vitro results demonstrated that the conjugation of mannose with the dendrimers significantly activated the internalization of the micromolecules in the course of the MR-mediated endocytosis. The investigation of absorption of the fluorescence-labeled dendrimers in the model of the rabbit intrauterine inflammation demonstrated that the mannose conjugation changed the dendrimer distribution along the whole rabbit body and resulted in an increase in the dendrimer number in the damaged glia of the brain. This system can probably be used for the addressed drug delivery to macrophages in the liver, lungs, brain, spleen, Langerhans dendritic skin cells, and others [85].

Dutta et al. [86] achieved an improvement of the therapeutic effect of a medicine due to mannosylation of the PPI-dendrimers (the analog, Fig. 12). The authors examined delivery of the efavirenz anti-HIV drug to the human monocytes and macrophages. The hemolytic activity and the cytotoxicity of the unmodified carrier were high, whereas the toxicity of the dendrimer that was conjugated with the mannose ligands proved to be insignificant. The starting dendrimer released the drug in vitro within 24 hours, but the modified carriers increased its action time to 144 hours. The significant improvement of the efavirenz absorption by monocytes and macrophages was observed in the case of the mannose-modified dendrimer (12 times higher than that of the free drug). The analogous PPI-dendrimers (Fig. 12) were prepared and examined by Kumar et al. [87]. The authors used the mannosylated dendrimers for the selective delivery of the rifampicin antituberculous drug to AMs. The

carrier modification resulted in an increase in the drug release from the dendrimer cavities and the AM absorption. The rifampicin concentration achieved 14.3 ng/mL (in comparison with that of 1.0 ng/mL in the case of the free medicine).

Thus, the mannose modification of the dendrimeric carriers enhances absorption of the drug carriers and the therapeutic potential and changes the biodistribution of the macromolecules in an organism for highly selective delivery.

An Application of Polyethylene Glycol (PEG) and Other Synthetic Polymeric Carriers

PEG is a common modifying agent which is also used for synthesis of different copolymers and changes in the surface properties and the circulation time of particles. The surface charge can affect the particle interaction with biological systems. A wide spectrum of PEG−chitosan copolymers (the modification degree of chitosan with PEG was 10−30%) with anionic liposomes was applied to the addressed delivery of doxorubicine to cells in the in vitro experiments [88, 89]. The PEG−chitosan copolymer was used for the liposomal stabilization (the protection against oxidation, membrane defects, and aggregation). The complex formation led to neutralization of the charge on the liposomes. The particle size was increased. The MTT tests for an evaluation of the metabolic activity of cells and the confocal microscopy demonstrated for the A459 and Caco-2 cellular lines of the human adenocarcinoma that liposomes covered with PEG-chi-

tosan had the same efficiency as the starting liposomes, but were much more stable and less toxic.

The better recognition of ligands by the mannose receptors could be achieved by the mannose modification of the PEG molecules [90, 91]. Raviv et al. [92] described structures and synthesis of the mannosylated polyionic complexes which consisted of polyethyleneimine (PEI, 25 kDa) and PEG (3.5 kDa) segments with Man and triMan residues as ligands for the targeting to MRs of DCs. The positively charged block-copolymers (Man-PEG-β-PEI and Man3-PEG-β-PEI) were prepared. The PEG fragment with the terminal mannose or trimannose residue was attached to the PEI polymer via a spacer. The Man_3-PEG-β-PEI polymers showed a three-four times higher transfection efficiency into dendritic cell lines (the THP-1 cells of the human monocytic leukemia and DC2.4 cells of the mouse monocytic leukemia) and showed a low cytotoxicity in comparison with Man-PEG-β-PEI polymers. The mannose-modified polymers demonstrated the higher efficiency (2—3 times) of the gene delivery to the CD11c$^+$ cells in comparison with the PEI—DNA complexes.

Gou et al. [93] achieved the higher parameters of the cellular absorption with the use of the copolymeric particles on the basis of PEG and ε-polylactide (57.5 kDa). The mannan-modified particles increased a concentration of immunoglobulins (IgG, IgG1, and IgG2a) in the mouse blood serum (C57BL/6) by 5—7 times in comparison with the unmodified particles. This fact was explained by the addressed targeting to DCs and activation of the humoral immunity.

D'Addio et al. [94] synthesized and applied copolymers of polystyrene (1.5 kDa) and PEG (5 kDa) with the terminal $-OCH_3$, $-OH$, or Man residues. The authors demonstrated with confocal fluorescence microscopy that the polymers with the terminal methoxygroups were not associated with the J774A and J774E mouse macrophages independently of the size of the particles. Specific targeting to MRs was studied with the use of carriers that involved 0—75% of the mannoside-terminal chains of PEG. The maximum association of the nanocarriers was achieved with 9% content of the chains with the mannose terminus; the absorption increased by more than three times in comparison with the nonmannosylated polymers.

Analysis of this article and the abovementioned papers demonstrates that the best results are achieved in the case of using the long-chain polymers, because the effect of multivalent binding occurs. A similar situation is observed for chitosan (see the section "IR-Fourier Spectroscopy: Attenuated Total Internal Reflection"). The most affine polymer should have a molecular mass >20—30 kDa.

Chen et al. [60] obtained the opposite dependence of the absorption on the chain length. They synthesized the PEG-containing nanoparticles (PEG—man-

nose residue—spacer—mannose residue—FITC) (Fig. 13a) for an evaluation of the influence of the number of the mannose units (Man), the carrier size (PEG), and the spacer length between neighboring mannose residues on particle absorption by the J774E MR-expressing mouse macrophages.

It was found using fluorescence and confocal spectroscopy that the $(Man)_2$-NC absorption was the highest among the nanoparticles with 0, 1, 2, or 4 mannose units. The compromise between the clusterization of the mannose residues and the steric hindrances was shown to be necessary. An optimum existed similarly to the previous paper where the maximum effect was achieved at 9%. The examined PEG-containing particles demonstrated the opposite dependence of the cellular absorption on the PEG molecular mass (5, 12, 20, 30, and 40 kDa). PEG with the molecular mass of 12 kDa was chosen for a study of the distance between the mannose residues. The three $(Man)_2$-PEG NC complexes with different distances between the mannose residues (39, 56, and 89 Å) were synthesized. The absorption of the nanoparticles with the 56-Å distance between the mannose residues proved to be four and two times higher than that of NC with the distances of 39 and 89 Å, respectively.

These results correlated with the data from [35]. Titov et al. [35] demonstrated that the presence of a spacer in the cyclodextin—mannose conjugates increased their affinity to ConA several times. In addition, the distance between the ConA binding sites was shown to be 68 Å (approximately the same distance as in CD206, see above), and this value was the closest to 56 Å ($(Man)_2$-PEG NC of the second type). Therefore, the proposal that the correspondence of the distance between the mannose residues in the polymer to that between the receptor sites increased the efficiency of ligand recognition was experimentally confirmed.

Thus, a definite optimum of the surface mannose modification exists for the nanoparticles and other drug carriers. Molecules with the required parameters can be synthesized using different ratios of polymers of different molecular masses.

Cyclodextrins

Cyclodextrins (CDs) are widely used carriers for medicines. CDs are cyclic glucose oligomers which are prepared by fermentation. They are distinguished according to the number of the glucose residues in one CD molecule. The simplest CD representatives are α-cyclodextrin, β-cyclodextrin, and γ-cyclodextrin. They contain six, seven, and eight glucopyranose units, respectively. The CD shape is a torus that looks like a hollow truncated cone. This shape is stabilized by hydrogen bonds between OH-groups and α-D-1,4-glycoside bonds. The CD hydroxyl groups are located on the outside surface of the molecule, and the internal cavity is hydrophobic and can form inclusion com-
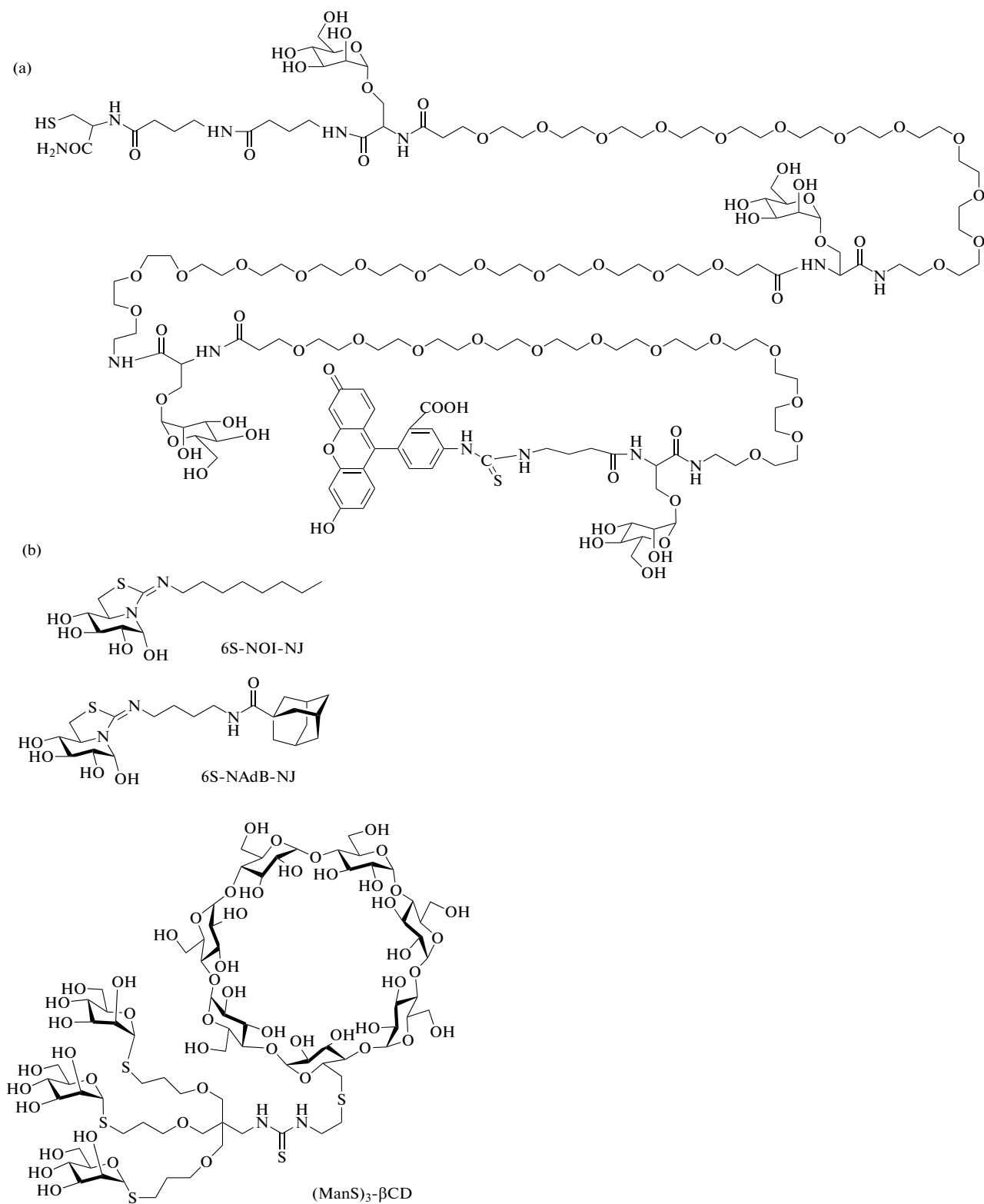
Fig. 13. (a) The structure of the mannosylated polymeric nanoparticles [60]; (b) the structures of the pharmacological 6S-NOI-NJ and 6S-NAdB-NJ chaperones and the (ManS)$_3$-βCD mannosylated cyclodextrin [97].

Table 4. The thermodynamic parameters and the dissociation constants (K_d) of the ConA system with (ManS)$_3$-βCD and the corresponding complexes with the 6S-NOI-NJ and 6S-NAdB-NJ pharmacological chaperones [97]

Molecule	Change in the energy during the complex formation, $\Delta G°$, kJ/mol	K_d of the complex, μM
(ManS)$_3$-βCD	-32.4 ± 1.0	2.1 ± 0.7
6S-NOI-NJ + (ManS)$_3$-βCD	-33.0 ± 3.1	1.6 ± 0.1
6S-NAdB-NJ + (ManS)$_3$-βCD	-31.0 ± 1.3	3.6 ± 1.5

plexes with other organic and inorganic molecules in aqueous solutions. Biologically active substances and medicines which are necessary to protect from an oxidation, hydrolysis, enzymatic destruction, excessive hygroscopicity, etc., are the "guest" molecules in the inclusion compounds. Therefore, CDs are widely used in the pharmaceutical industry. Their most important properties are an increase in a solubility of therapeutic agents in water due to the hydrophilic external envelope and an enhancement of the drug penetration through biological membranes.

Many CD conjugates are described in the literature. Let us discuss the most promising conjugates. Gómez-García et al. [95] synthesized heteroglycoclusters with a central cyclodextrin. They examined various CD modifications by carbohydrates (Man, Glc, and Lac). CD with three mannose residues exhibited the highest affinity to ConA. The lectin affinity was increased in 7 times in comparison with MeMan.

Yuan et al. [96] proposed an interesting and promising compound on the basis of the dextrin-modified chitosan (CD-Chit) as a new carrier for poorly water-soluble therapeutic agents. The polymer was prepared from chitosan (110 kDa) and mono-6-deoxy-6-(n-toluenesulfonyl)-β-CD with the substitution degree of 10−20%. A possibility of a synthesis of particles with a wide range of the desired parameters was demonstrated: a size of 202−589 nm and the ζ-potential from +23 to +43 mV. These characteristics were important for a choice of the optimal carrier for medicines. The encapsulation efficiency of ketoprofen into the chitosan nanoparticles with 20% CD was 1.36 times higher than that of the unmodified polymer. The rate and time of a release of ketoprofen from the nanoparticles was controlled by pH and the CD quantity. Thus, Chit-CD could be used as a biodegraded system of a delivery of poorly water-soluble medicines with regulated parameters of the release of a drug and, hence, a fixed action on the target cells.

The properties of the mannose-containing CD-carrier and its complex with the 6S-NOI-NJ and 6S-NAdB-NJ chaperone proteins (in this case, these proteins were used for the treatment of the Gaucher's disease) were studied [97]. A comparative investigation of the ConA binding ability of (ManS)$_3$-β-CD (the mannose residues were connected through the spacer, Fig. 13b) and the corresponding complexes with the proteins was performed by isothermal titration calorimetry in order to examine the targeting to the mannose-specific lectins. The changes in the Gibbs energy during the complex formation between ConA and CD and its conjugates were determined (Table 4). A stoichiometry of the complexes was 1 : 1, i.e., the mannosylated dendron in (ManS)$_3$-β-CD interacted with only one ConA subunit. An inclusion of the chaperone in the β-CD cavity did not significantly affect the lectin affinity. The results suggested a two-order enhancement of the affinity of the cyclodextrin carrier in comparison with methyl-α-D-mannopyranoside (K_d = 156 μM). Thus, the three-valent mannose residue in the (ManS)$_3$-β-CD carrier was effectively recognized by the lectin receptors. The recognition was dozens of times better than that of mannopyranoside due to the multivalent effect. The cyclodextrin system was also characterized by the optimal parameters of the incorporation of the target substance.

Titov et al. [35] reviewed the large number of the drug carriers on the basis of CDs and discussed the basic methods for preparation of monodendated and oligodendated glycoconjugates based on cyclocarbohydrate matrixes and their interaction with lectins, including the mannose glycoconjugates. The interaction of the oligosaccharide ligands with lectins itself is relatively weak (K_d = 10^{-6}−10^{-3} M). The low efficiency of the single interactions is compensated by an increase in their quantity owing to clusterization of many copies of carbohydrate ligands and their receptors. As a result, more stable cooperative binding occurs due to the cluster effect. This effect is taken into account during a creation of novel classes of the carbohydrate-containing medicines. Glycoconjugates are 16−17 times more effective than methyl-α-mannopyranoside owing to the cluster effect and the spacer application. The hepta-valent conjugate with C$_5$-CD spacers proves to be 40 times more active than CDs with the mannose residues without spacers. Therefore, a definite spatial arrangement of the lectin ligands is important for the process of the glycoconjugate−lectin binding. These data are confirmed by the dependences of structures and K_d of the complexes of the mannose oligopeptides with ConA (see the subsection "Fluorescence Spectroscopy") (Table 2). The mutual position of monomers in an oligosaccharide has a determining importance.

Titov et al. [35] described series of in vivo experiments to determine the ability of the CD-mannose glycol cluster to stimulate the MPh RAW 264.7 cellular line for production of the TNF-α inflammatory cytokine. Measurements of the fluorescence intensity demonstrated that the conjugate was bound to the MPh plasmatic membrane. The conjugate in a concentration of 400 μg/mL stimulated formation of TNF-α at approximately the same level as lipopolysaccharide that modeled the bacterial surface. Thus, a therapeutic potential of the CD-Man conjugate was demonstrated.

CONCLUSIONS

One can conclude from the aforementioned examples that the use of the mannosylated compounds for the addressed drug delivery by the targeting to the macrophage MRs is a promising strategy for treatment of various diseases. Variation of the mannosylation degree or the ratio of components in a conjugate presents the possibility of regulating pharmacokinetic parameters and the biodistrubution of a carrier with a medicine throughout an organism. An example of the effective carrier is β-cyclodextrin with seven residues of 3,6-di-*O*-(β(1,2)-GlcNAc-mannopyranosyl)-α-mannopyranose which are connected via spacers so that the distance between the mannose residues approximately corresponds to the distance in the ConA binding sites. Such carriers increase the specificity to the mannose receptors by dozens of times owing to the optimal clusterization of the Man residues. An application of the nanoparticles from biodegraded polymers and the ligands that provide the directed action opens up possibilities for creating novel therapeutic forms with a prolonged action and addressed delivery. Such new constructs allow a decrease in a load of therapeutic agents on an organism and their toxicity, a considerable shortening of the treatment time, a significant decrease in antibiotic resistance, and, as a result, an improvement of treatment efficiency.

COMPLIANCE WITH ETHICAL STANDARDS

Conflict of Interests

The authors declare that they have no conflicts of interests.

This article does not contain any studies involving humans and animals performed by any of the authors.

REFERENCES

1. Pittet, M.J., Nahrendorf, M., and Swirski, F.K., *Ann. N.Y. Acad. Sci.*, 2014, vol. 1319, pp. 1−18.
https://doi.org/10.1111/nyas.12393

2. Allard, B., Panariti, A., and Martin, J.G., *Front. Immunol.*, 2018, vol. 9, pp. 1777−1783.
https://doi.org/10.3389/fimmu.2018.01777

3. Yuk, J.-M. and Jo, E.-K., *J. Bacteriol. Virol.*, 2011, vol. 41, pp. 225−235.
https://doi.org/10.4167/jbv.2011.41.4.225

4. Cambi, A. and Figdor, C., *Curr. Biol.*, 2009, vol. 19, pp. 375−378.
https://doi.org/10.1016/j.cub.2009.03.032

5. Dheda, K., Schwander, S.K., Zhu, B., van Zyl-Smit, R.N., and Zhang, Y., *Respirol.*, 2010, vol. 15, pp. 433−450.
https://doi.org/10.1111/j.1440-1843.2010.01739.x

6. Taylor, P.R., Martinez-Pomares, L., Stacey, M., Lin, H.-H., Brown, G.D., and Gordon, S., *Annu. Rev. Immunol.*, 2005, vol. 23, pp. 901−944.
https://doi.org/10.1146/annurev.immunol.23.021704.115816

7. Yonekawa, A., Saijo, S., Hoshino, Y., Miyake, Y., Ishikawa, E., Suzukawa, M., and Yamasaki, S., *Immunity*, 2014, vol. 41, pp. 402−413.
https://doi.org/10.1016/j.immuni.2014.08.005

8. Ezekowitz, R.A., Sastry, K., Bailly, P., and Warner, A., *J. Exp. Med.*, 1990, vol. 172, pp. 1785−1794.
https://doi.org/10.1084/jem.172.6.1785

9. Filatova, L.Y., Klyachko, N.L., and Kudryashova, E.V., *Russ. Chem. Rev.*, 2018, vol. 87, pp. 374−391.
https://doi.org/10.1070/rcr4740

10. Martínez-Pomares, L., Mahoney, J.A., Káposzta, R., and Linehan, S.A., *J. Biol. Chem.*, 1998, vol. 273, pp. 23376−23380.
https://doi.org/10.1074/jbc.273.36.23376

11. East, L. and Isacke, C.M., *Biochim. Biophys. Acta*, 2002, vol. 1572, pp. 364−386.
https://doi.org/10.1016/S0304-4165(02)00319-7

12. Leteux, C., Chai, W., Loveless, R.W., and Yuen, C.T., *J. Exp. Med.*, 2000, vol. 191, pp. 1117−1126.
https://doi.org/10.1084/jem.191.7.1117

13. Feinberg, H., Jégouzo, S.A.F., Lasanajak, Y., Smith, D.F., Drickamer, K., Weis, W.I., and Taylor, M.E., *J. Biol. Chem.*, 2021, vol. 296, pp. 100368−100385.
https://doi.org/10.1016/j.jbc.2021.100368

14. Drickamer, K., *Curr. Opin. Struct. Biol.*, 1999, vol. 9, pp. 585−590.
https://doi.org/10.1016/S0959-440X(99)00009-3

15. Napper, C.E., Drickamer, K., and Taylor, M.E., *Biochem. J.*, 2006, vol. 395, no. 3, pp. 579−586.
https://doi.org/10.1042/bj20052027

16. Fiete, D.J., Beranek, M.C., and Baenziger, J.U., *Proc. Natl. Acad. Sci. U. S. A.*, 1998, vol. 95, pp. 2089−2093.
https://doi.org/10.1073/pnas.95.5.2089

17. Liu, Y., Chirino, A.J., Misulovin, Z., Leteux, C., Feizi, T., Nussenzweig, M.C., and Bjorkman, P.J., *J. Exp. Med.*, 2000, vol. 191, pp. 1105−1116.
https://doi.org/10.1084/jem.191.7.1105

18. Feinberg, H., Park-Snyder, S., Kolatkar, A.R., Heise, C.T., Taylor, M.E., and Weis, W.I., *J. Biol. Chem.*, 2000, vol. 275, pp. 21539−21548.
https://doi.org/10.1074/jbc.M002366200

19. Taylor, M.E. and Drickamer, K., *J. Biol. Chem.*, vol. 268, pp. 399−404.
https://doi.org/10.1016/s0021-9258(18)54164-8

20. Mullin, N.P., Hail, K.T., and Taylor, M.E., *J. Biol. Chem.*, 1994, vol. 269, pp. 28405−28413.
https://doi.org/10.1016/S0021-9258(18)46942-6

21. Weis, W.I. and Drickamer, K., *Annu. Rev. Biochem.*, 1996, vol. 65, pp. 441−473.
https://doi.org/10.1146/annurev.bi.65.070196.002301

22. Weis, W.I., Drickamer, K., and Hendrickson, W.A., *Nature*, 1992, vol. 360, pp. 127−134.
https://doi.org/10.1038/360127a0

23. Sheriff, S., Chang, C., and Ezekowitz, R., *Nat. Struct. Mol. Biol.*, 1994, vol. 1, pp. 789−794.
https://doi.org/10.1038/nsb1194-789

24. Thiel, S., Vorup-Jensen, T., Stover, C., Schwaeble, W., Laursen, S.B., Poulsen, K., Willis, A.C., Eggleton, P., Hansen, S., Holmskov, U., Reid, K.B.M., and Jensenius, J.C., *Nature*, 1997, vol. 386, pp. 506−510.
https://doi.org/10.1038/386506a0

25. Suzuki, Y., Shirai, M., and Asada, K., *Sci. Rep.*, 2018, vol. 8, p. 13129.
https://doi.org/10.1038/s41598-018-31565-5

26. Mazlan, M.K.N., Tazizi, M.H.D., Ahmad, R., Noh, M.A.A., Bakhtiar, A., Wahab, H.A., and Gazzali, A., *Antibiotics*, 2021, vol. 10, p. 908.
https://doi.org/10.3390/antibiotics10080908

27. Liener, I.E., Sharon, N., and Goldstein, I.J., *The Lectins Properties, Functions and Applications in Biology and Medicine*, Orlando: Academic, 1986.

28. Loris, R., Hamelryck, T., Bouckaert, J., and Wyns, L., *Biochim. Biophys. Acta*, 1998, vol. 1383, pp. 9−36.
https://doi.org/10.1016/S0167-4838(97)00182-9

29. Olson, M.O.J. and Liener, I.E., *Biochemistry*, 1967, vol. 6, pp. 105−111.
https://doi.org/10.1021/bi00853a018

30. Senear, D.F. and Teller, D.C., *Biochemistry*, 1981, vol. 20, pp. 3083−3091.
https://doi.org/10.1021/bi00514a015

31. Brewer, C.F., Brown, R.D., and Koenig, S.H., *J. Biomol. Str. Dyn.*, 1983, vol. 1, pp. 961−997.
https://doi.org/10.1080/07391102.1983.10507497

32. Kaushik, S., Mohanty, D., and Surolia, A., *Biophys. J.*, 2009, vol. 96, pp. 21−34.
https://doi.org/10.1529/biophysj.108.134601

33. Naismith, J.H., Emmerich, C., Habash, J., Harrop, S.J., Helliwell, J.R., Hunter, W.N., and Yariv, J., *Acta Crystallogr., Sect. D: Biol. Crystallogr.*, 1994, vol. 50, pp. 847−858.
https://doi.org/10.1107/s0907444994005287

34. Le-Deygen, I.M., Mamaeva, P.V., Skuredina, A.A., and Kudryashova, E.V., *Moscow Univ. Chem. Bull.*, 2020, vol. 75, pp. 213−217.
https://doi.org/10.3103/S0027131420040045

35. Titov, D.V., Gening, M.L., Tsvetkov, Yu.E., and Nifantiev, N.E., *Russ. J. Bioorg. Chem.*, 2013, vol. 39, pp. 451−487.
https://doi.org/10.1134/S1068162013050142

36. Naismith, J.H. and Field, R.A., *J. Biol. Chem.*, 1996, vol. 271, pp. 972−976.
https://doi.org/10.1074/jbc.271.2.972

37. Gerlits, O.O., Coates, L., Woods, R.J., and Kovalevsky, A., *Biochemistry*, 2017, vol. 56, pp. 4747−4750.
https://doi.org/10.1021/acs.biochem.7b00654

38. Sukumaran, S., *Protein Secondary Structure Elucidation Using FTIR Spectroscopy*, Thermo Fisher Scientific. Inc. BioCell, 2018.

39. Kudryashova, E.V., *Funktsionirovanie i struktura belkov na poverkhnostyakh razdela faz. Novye metody issledovaniya* (*Functioning and Structure of Proteins at Interfaces: New Research Methods*), Moscow: Palmarium Acad. Publ., 2013, pp. 1−146.

40. Itagaki, H., Fluorescence spectroscopy, in *Experimental Methods in Polymer Science: Modern Methods in Polymer Research and Technology*, Tanaka, T., Ed., Academic Press, 2000, pp. 155−260.

41. Visser, A.J.W.G., Van der Berg, P.A.W., Visser, N.V., van Hoek, A., Burg, H.A., Parsonage, D., and Claiborne, A., *J. Phys. Chem. B*, 1998, vol. 102, pp. 10431−10439.
https://doi.org/10.1021/jp982141h

42. Lakowicz, J.R., *Principles of Fluorescence Spectroscopy*, Springer-Verlag US, 1999.
https://doi.org/10.1007/978-1-4757-3061-6

43. Kudryashova, E.V., Gladilin, A.K., and Levashov, A.V., *Usp. Biol. Khim.*, 2002, vol. 42, pp. 257−294.

44. Landshcoot, A., Loontiens, F.G., and De Bruyne, C.K., *Eur. J. Biochem.*, 1978, vol. 83, pp. 277−285.
https://doi.org/10.1111/j.1432-1033.1978.tb12092.x

45. Landschoot, A., Loontiens, F.G., and De Bryune, C.K., *Eur. J. Biochem.*, 1980, vol. 103, pp. 307−312.
https://doi.org/10.1111/j.1432-1033.1980.tb04316.x

46. Yuasa, H., Kamata, Y., Kurono, S., and Hashimoto, H., *Bioorg. Med. Chem. Lett.*, 1998, vol. 8, pp. 2139−2144.
https://doi.org/10.1016/S0960-894X(98)00364-3

47. Mandal, D.K., Kishore, N., and Brewer, C.F., *Biochemistry*, 1994, vol. 33, pp. 1149−1156.
https://doi.org/10.1021/bi00171a014

48. Dam, T.K., Roy, R., Das, S.K., Oscarson, S., and Brewer, C.F., *J. Biol. Chem.*, 2000, vol. 275, pp. 14223−14230.
https://doi.org/10.1074/jbc.275.19.14223

49. Maverakis, E., Kim, K., Shimoda, M., Gershwin, M.E., Patel, F., Wilken, R., Raychaudhuri, S., Ruhaak, L.R., and Lebrilla, C.B., *J. Autoimmun.*, 2015, vol. 57, pp. 1−13.
https://doi.org/10.1016/j.jaut.2014.12.002

50. Aizpurua-Olaizola, O., Torano, J.S., Pukin, A., Fu, O., Boons, G.J., de Jong, G.J., and Pieters, R.J., *Electrophoresis*, 2018, vol. 39, pp. 344−347.

51. Introduction to Affinity Chromatography. www.bio-rad.com/ru-ru/applications-technologies/introduction-affinity-chromatography?ID=MWHAVG4VY.

52. Hage, D., *Clin. Chem.*, 1999, vol. 45, pp. 593−615.
https://doi.org/10.1093/clinchem/45.5.593

53. Freeze, H.H., *Curr. Protocols Prot. Sci.*, 1995, pp. 9.1.1−9.1.9.
https://doi.org/10.1002/0471140864.ps0901s00

54. Bekker, Yu., *Khromatografiya. Instrumental'naya analitika. Metody khromatografii i kapillyarnogo elektroforeza* (Chromatography. Instrumental Analytics. Chromatography and Capillary Electrophoresis Methods), Moscow: Tekhnosfera, 2009.

55. Argayosa, A.M., Bernal, R.A.D., Luczon, A.U., and Arboleda, J.S., *Aquaculture*, 2011, vol. 310, pp. 274−280.
https://doi.org/10.1016/j.aquaculture.2010.11.002

56. Andon, N.L., Eckert, D., Yates, J.R., and Haynes, P.A., *Proteomics*, 2003, vol. 3, pp. 1270−1278.
https://doi.org/10.1002/pmic.200300447

57. Pawley, J.B., *Handbook of Biological Confocal Microscopy*, 3rd ed., Berlin: Springer, 2006.

58. Wilson, T., *Confocal Microscopy. Encyclopedia of Modern Optics*, London: Academic, 2005.

59. Ghotbi, Z., Haddadi, A., Hamdy, S., Hung, R.W., Samuel, J., and Lavasanifar, A., *J. Drug Target*, 2010, vol. 19, pp. 281−292.
https://doi.org/10.3109/1061186X.2010.499463

60. Chen, P., Zhang, X., Jia, L., Prud'homme, R.K., Szekely, Z., and Sinko, P.J., *J. Controlled Release*, 2014, vol. 194, pp. 341−349.
https://doi.org/10.1016/j.jconrel.2014.09.006

61. Picot, J., Guerin, C.L., Le Van Kim, C., and Boulanger, C.M., *Cytotechnology*, 2012, vol. 64, pp. 109−130.
https://doi.org/10.1007/s10616-011-9415-0

62. Givan, A.L., in *Flow Cytometry Protocols*, Methods Mol. Biol. (Methods and Protocols), Hawley, T. and Hawley, R., Eds., Humana Press, 2011, vol. 699.
https://doi.org/10.1007/978-1-61737-950-5_1

63. Roederer, M., *Cytometry*, 2001, vol. 45, pp. 194−205.
https://doi.org/10.1002/1097-0320(20011101)45:3<194::AID-CYTO1163>3.0.CO;2-C

64. Ying, W., Cheruku, P.S., Bazer, F.W., Safe, S.H., and Zhou, B., *J. Vis. Exp.*, 2013, vol. 76, pp. 50323−50330.
https://doi.org/10.3791/50323

65. Gordon, S., *Nat. Rev. Immunol.*, 2003, vol. 3, pp. 23−35.
https://doi.org/10.1038/nri978

66. Arkan, M.C., Hevener, A.L., Greten, F.R., Maeda, S., Li, Z.W., Long, J.M., Wynshaw-Boris, A., Poli, G., Olefsky, J., and Karin, M., *Nat. Med.*, 2005, vol. 11, pp. 191−198.
https://doi.org/10.1038/nm1185

67. Rapoport, E.M., Sapot'ko, Y.B., Pazynina, G.V., Bojenko, V.K., and Bovin, N.V., *Biochemistry* (Moscow), 2005, vol. 70, pp. 330−338.
https://doi.org/10.1007/s10541-005-0119-y

68. Cornish, A.L., Freeman, S., Forbes, G., Ni, J., Zhang, M., Cepeda, M., Gentz, R., Augustus, M., Carter, K.C., and Crocker, P.R., *Blood*, 1998, vol. 92, pp. 2123−2132.
https://doi.org/10.1182/blood.V92.6.2123

69. Barkal, A.A., Brewer, R.E., Markovic, M., Kowarsky, M., Barkal, S.A., Zaro, B.W., Krishnan, V., Hatakeyama, J., Dorigo, O., Barkal, L.J., and Weissman, I.L., *Nature*, 2019, vol. 572, pp. 392−396.
https://doi.org/10.1038/s41586-019-1456-0

70. Mantuano, N., Natoli, M., Zippelius, A., and Laubli, H., *J. ImmunoTher. Cancer*, 2020, vol. 8, art. e001222.
https://doi.org/10.1136/jitc-2020-001222

71. Satoh, T., Suzuki, K., Yamaguchi, T., and Kato, K., *PLoS One*, 2014, vol. 9, art. e87963.
https://doi.org/10.1371/journal.pone.0087963

72. Moothoo, D.N., Canan, B., Field, R.A., and Naismith, J.H., *Glycobiology*, 1999, vol. 9, pp. 539−545.
https://doi.org/10.1093/glycob/9.6.539

73. Freichels, H., Wagner, M., Okwieka, P., Meyer, R.G., Mailander, V., Landfester, K., and Musyanovych, A.,
J. Mater. Chem. B, 2013, vol. 1, pp. 4338−4348.
https://doi.org/10.1039/C3TB20138D

74. Monsigny, M., Roche, A.C., Midoux, P., and Mayer, R., *Adv. Drug Deliv. Rev.*, 1994, vol. 14, pp. 1−24.
https://doi.org/10.1016/0169-409X(94)90003-5

75. Garg, M. and Jain, N.K., *J. Drug Target*, 2006, vol. 14, pp. 1−11.
https://doi.org/10.1080/10611860500525370

76. Chono, S., Kaneko, K., Yamamoto, E., Togami, K., and Morimoto, K., *Drug Dev. Ind. Pharm.*, 2010, vol. 36, pp. 102−107.
https://doi.org/10.3109/03639040903099744

77. Kawakami, S., Sato, A., Nishikawa, M., Yamashita, F., and Hashida, M., *Gene Ther.*, 2000, vol. 7, pp. 292−299.
https://doi.org/10.1038/sj.gt.3301089

78. Wijagkanalan, W., Kawakami, S., Takenaga, M., Igarashi, R., Yamashita, F., and Hashida, M., *J. Controlled Release*, 2008, vol. 125, pp. 121−130.
https://doi.org/10.1016/j.jconrel.2007.10.011

79. Nimje, N., Agarwal, A., Saraogi, G.K., Lariya, N., Rai, G., Agrawal, H., and Agrawal, G.P., *J. Drug Target*, 2009, vol. 17, pp. 777−787.
https://doi.org/10.3109/10611860903115308

80. Grenha, A., Al-Qadi, S., Seijo, B., and Remunan-Lopez, C., *J. Drug Deliv. Sci. Technol.*, 2010, vol. 20, pp. 33−43.
https://doi.org/10.1016/S1773-2247(10)50004-2

81. Chung, Y.C., Tsai, C.F., and Li, C.F., *Fish. Sci.*, 2006, vol. 72, pp. 1096−1103.
https://doi.org/10.1111/j.1444-2906.2006.01261.x

82. Il'ina, A.V., Kulikov, S.N., Chalenko, G.I., Gerasimova, N.G., and Varlamov, V.P., *App. Biochem. Microbiol.*, 2008, vol. 44, pp. 551−558.
https://doi.org/10.1134/S0003683808050177

83. Asthana, G.S., Asthana, A., Kohli, D.V., and Vyas, S.P., *BioMed Res. Int.*, 2014, vol. 2014, pp. 1−17.
https://doi.org/10.1155/2014/526391

84. Budzynska, R., Nevozhay, D., Kanska, U., Jagiello, M., Opolski, A., Wietrzyk, J., and Boratynski, J., *Oncol. Res.*, 2007, vol. 16, pp. 415−421.
https://doi.org/10.3727/000000007783980837

85. Sharma, A., Porterfield, J.E., Smith, E., Sharma, R., Kannan, S., and Kannan, R.M., *J. Controlled Release*, 2018, vol. 283, pp. 175−189.
https://doi.org/10.1016/j.jconrel.2018.06.003

86. Dutta, T., Agashe, H.B., Garg, M., Balasubramanium, P., Kabra, M., and Jain, N.K., *J. Drug Target*, 2007, vol. 15, pp. 89−98.
https://doi.org/10.1080/10611860600965914

87. Kumar, P.V., Asthana, A., Dutta, T., and Jain, N.K., *J. Drug Target*, 2006, vol. 14, pp. 546−556.
https://doi.org/10.1080/10611860600825159

88. Le-Deygen, I.M. and Kudryashova, E.V., *Moscow Univ. Chem. Bull.*, 2018, vol. 73, pp. 69−73.
https://doi.org/10.3103/S0027131418020074

89. Deygen, I.M., Seidl, C., Kolmel, D.K., Kudryashova, E.V., Brase, S., and Schepers, U., *Langmuir*, 2016, vol. 32, pp. 10861−10869.
https://doi.org/10.1021/acs.langmuir.6b01023

90. Parveen, S. and Sahoo, S., *Clin. Pharmacokinet.*, 2006, vol. 45, pp. 965−988.
https://doi.org/10.2165/00003088-200645100-00002

91. Rajan, M. and Raj, V., *Int. J. Pharm. Pharm. Sci.*, 2012, vol. 4, p. 255.
https://doi.org/10.1016/j.ijpharm.2013.06.030

92. Raviv, L., Jaron-Mendelson, M., and David, A., *Mol. Pharm.*, 2015, vol. 12, pp. 453−462.
https://doi.org/10.1021/mp5005492

93. Gou, M.L., Dai, M., Li, X., Yang, L., Huang, M., Wang, Y., Kan, B., Lu, Y., Wei, Y., and Qian, Z., *Colloids Surf.*, 2008, vol. 64, pp. 135−139.
https://doi.org/10.1016/j.colsurfb.2007.12.014

94. D'Addio, S.M., Baldassano, S., Shi, L., Cheung, L., Adamson, D.H., Bruzek, M., Anthony, J.E., Laskin, D.L., Sinko, P.J., and Prud'homme, R.K., *J. Controlled Release*, 2013, vol. 168, pp. 41−49.
https://doi.org/10.1016/j.jconrel.2013.02.004

95. Gómez-García, M., Benito, J.M., Rodríguez-Lucena, D., Yu, J.-X., Chmurski, K., Mellet, C.O., Gallego, R.G., Maestre, A., Defaye, J., and Fernández, J.M.G., *J. Am. Chem. Soc.*, 2005, vol. 127, pp. 7970−7971.
https://doi.org/10.1021/ja050934t

96. Yuan, Z., Ye, Y., Gao, F., Yuan, H., Lan, M., Lou, K., and Wang, W., *Int. J. Pharm.*, 2013, vol. 446, pp. 191−198.
https://doi.org/10.1016/j.ijpharm.2013.02.024

97. Rodríguez-Lavado, J., de la Mata, M., Jiménez-Blanco, J.L., García-Moreno, M.I., Benito, J.M., Díaz-Quintana, A., Sánchez-Alcázar, J.A., Higaki, K., Nanba, E., Ohno, K., Suzuki, Y., Mellet, C.O., and García Fernández, J.M., *Org. Biomol. Chem.*, 2014, vol. 12, pp. 2289−2301.
https://doi.org/10.1039/C3OB42530D

Translated by L. Onoprienko